

4 The Precambrian paleogeography of Laurentia

Nicholas L. Swanson-Hysell¹

¹ Department of Earth and Planetary Science, University of California, Berkeley, CA 94720 USA

This chapter is in preparation for the book Ancient Supercontinents and the Paleogeography of the Earth

¹ 4.1 Abstract

Laurentia is the craton that forms the Precambrian core of North America and was a major continent throughout the majority of the Proterozoic. The paleogeographic position of Laurentia is key to the development of reconstructions of Proterozoic paleogeography including the Paleoproterozoic-Mesoproterozoic Nuna and Neoproterozoic Rodinia supercontinents. There is a rich record of Precambrian paleomagnetic poles from Laurentia, as well as an extensive and well-documented geologic history of tectonism. These geologic and paleomagnetic records are increasingly better constrained geochronologically and are both key to evaluating and developing paleogeographic models. These data from Laurentia provides strong-support for mobile lid plate tectonic processes operating continuously over the past 2.2 billion years.

¹¹ 4.2 Introduction and broad tectonic history

Laurentia refers to the craton that forms the Precambrian interior of North America and Greenland (Fig. 1). Laurentia comprises multiple Archean provinces that had unique histories prior to their amalgamation in the Paleoproterozoic, as well as tectonic zones of crustal growth that post-date this assembly (Hoffman, 1989; Whitmeyer and Karlstrom, 2007). Collision between the Superior province and the composite Slave+Rae+Hearne provinces that resulted in the Trans-Hudson orogeny represents a major event in the formation of Laurentia (Corrigan et al., 2009). Terminal collision recorded in the Trans-Hudson orogen is estimated to have been ca. 1.86 to 1.82 Ga based on constraints such as U-Pb dating of monazite grains and zircon rims (Skipton

20 et al., 2016; Weller and St-Onge, 2017, e.g.). A period of accretionary and collisional orogenesis is
21 recorded in the constituent provinces and terranes of Laurentia leading up to the terminal
22 collision of the Trans-Hudson orogeny. This overall story of rapid Paleoproterozoic amalgamation
23 of Laurentia's constituent Archean provinces, including the terminal Trans-Hudson orogeny, was
24 synthesized in the seminal *United Plates of America* paper of Hoffman (1988) and has been
25 refined in the time since – particularly with additional geochronological constraints. Of most
26 relevance here are the events that led to the suturing of more major Archean provinces: the
27 Thelon orogen associated with the collision between the Slave and Rae provinces ca. 2.0 to 1.9 Ga
28 (Hoffman, 1989); the Snowbird orogen associated with ca. 1.89 Ga collision between the Rae and
29 Hearne provinces and associated terranes (Berman et al., 2007); the Nagssugtoqidian orogen due
30 to the ca. 1.86 to 1.84 Ga collision between the Rae and North Atlantic provinces (St-Onge et al.,
31 2009); and the Torngat orogen resulting from the ca. 1.87 to 1.85 Ga collision of the Meta
32 Incognita province (grouped with the Rae province in older compilations) with the North Atlantic
33 province (St-Onge et al., 2009).

34 As for the suturing of the Wyoming province to Laurentia, many models posit that it was
35 conjoined with Hearne and associated provinces at the time of the Trans-Hudson orogeny (e.g.
36 St-Onge et al., 2009; Pehrsson et al., 2015) or was proximal to Hearne and Superior while still
37 undergoing continued translation up to ca. 1.80 Ga (Whitmeyer and Karlstrom, 2007). A
38 contrasting view has been proposed that the Wyoming province and Medicine Hat blocks
39 were not conjoined with the other Laurentia provinces until ca. 1.72 Ga (Kilian et al., 2016). This
40 interpretation is argued to be consistent with geochronological constraints on monazite and
41 metamorphic zircon indicating active collisional orogenesis associated with the Big Sky orogen on
42 the northern margin of the craton as late as ca. 1.75 to 1.72 Ga (Condit et al., 2015) and ca. 1.72
43 tectonomagmatic activity in the Black Hills region (Redden et al., 1990). However, the evidence
44 for earlier orogenesis ca. 1.78 to 1.75 in the Black Hills (Dahl et al., 1999; Hrncir et al., 2017), as
45 well as high-grade metamorphism as early as ca. 1.81 Ga in the Big Sky orogen (Condit et al.,
46 2015), may support the interpretation of Hrncir et al. (2017) that ca. 1.72 Ga activity is a minor
47 overprint on ca. 1.75 terminal suturing between Wyoming and Superior. Regardless, in both of
48 these interpretations, Wyoming is a later addition to Laurentia with final suturing post-dating ca.

49 1.82 Ga amalgamation of Archean provinces with the Trans-Hudson orogen further to the
50 northeast. Overall, the collision of these Archean microcontinents between ca. 1.9 and 1.8 Ga led
51 to rapid amalgamation of the majority of the Laurentia craton (Fig. 1).

52 Crustal growth also progressed in the Paleoproterozoic through accretionary orogenesis. This
53 accretion occurred within the Wopmay orogen through ca. 1.88 Ga arc-continent collision that led
54 to the accretion of the Hottah terrane (the Calderian orogeny) and the subsequent emplacement
55 of the Great Bear magmatic zone from ca. 1.88 to 1.84 Ga (Hildebrand et al., 2009). Coeval with
56 the Trans-Hudson orogeny was the peripheral Penokean orogeny during which both
57 microcontinent blocks (the Marshfield terrane) and arc terranes accreted on the southeastern
58 margin of the west Superior province ca. 1.86 to 1.82 (Schulz and Cannon, 2007). Firm evidence
59 of the end of the orogeny comes from the ca. 1.78 undeformed plutons of the post-Penokean East
60 Central Minnesota Batholith (Holm et al., 2005).

61 The collisions of provinces and terranes leading up to the Trans-Hudson orogeny mark the
62 initial phase of assembly of the supercontinent Nuna in the paleogeographic model framework of
63 Pehrsson et al. (2015). The Trans-Hudson orogeny itself is taken to be the terminal collision
64 associated with the closure of the Manikewan Ocean that had previously been a large oceanic
65 tract separating the Superior province from the composite Slave+Rae+Hearne+North Atlantic
66 provinces (often referred to as the Churchill domain or plate; e.g. Skipton et al., 2016; Weller and
67 St-Onge, 2017; Fig. 4). The paleogeographic mode of Pehrsson et al. (2015) posits that this
68 period of terminal collision not only resulted in the amalgamation of Laurentia, but was also
69 associated with the assembly of the supercontinent Nuna that is hypothesized to include other
70 major Paleoproterozoic cratons including Baltica, Siberia, Congo/São Francisco, West Africa, and
71 Amazonia.

72 Following the Trans-Hudson orogeny, the locus of orogenesis migrated to the exterior of
73 Laurentia. This change marks a shift in the predominant style of Laurentia's growth as
74 subsequent crustal growth occurred dominantly through accretion of juvenile crust along the
75 southern and eastern margin of the nucleus of Archean provinces (Whitmeyer and Karlstrom,
76 2007; Figs. 1 and 2). Determining the extent of these belts is complicated by poor exposure of
77 them in the midcontinent relative to the exposure of the Archean provinces throughout the

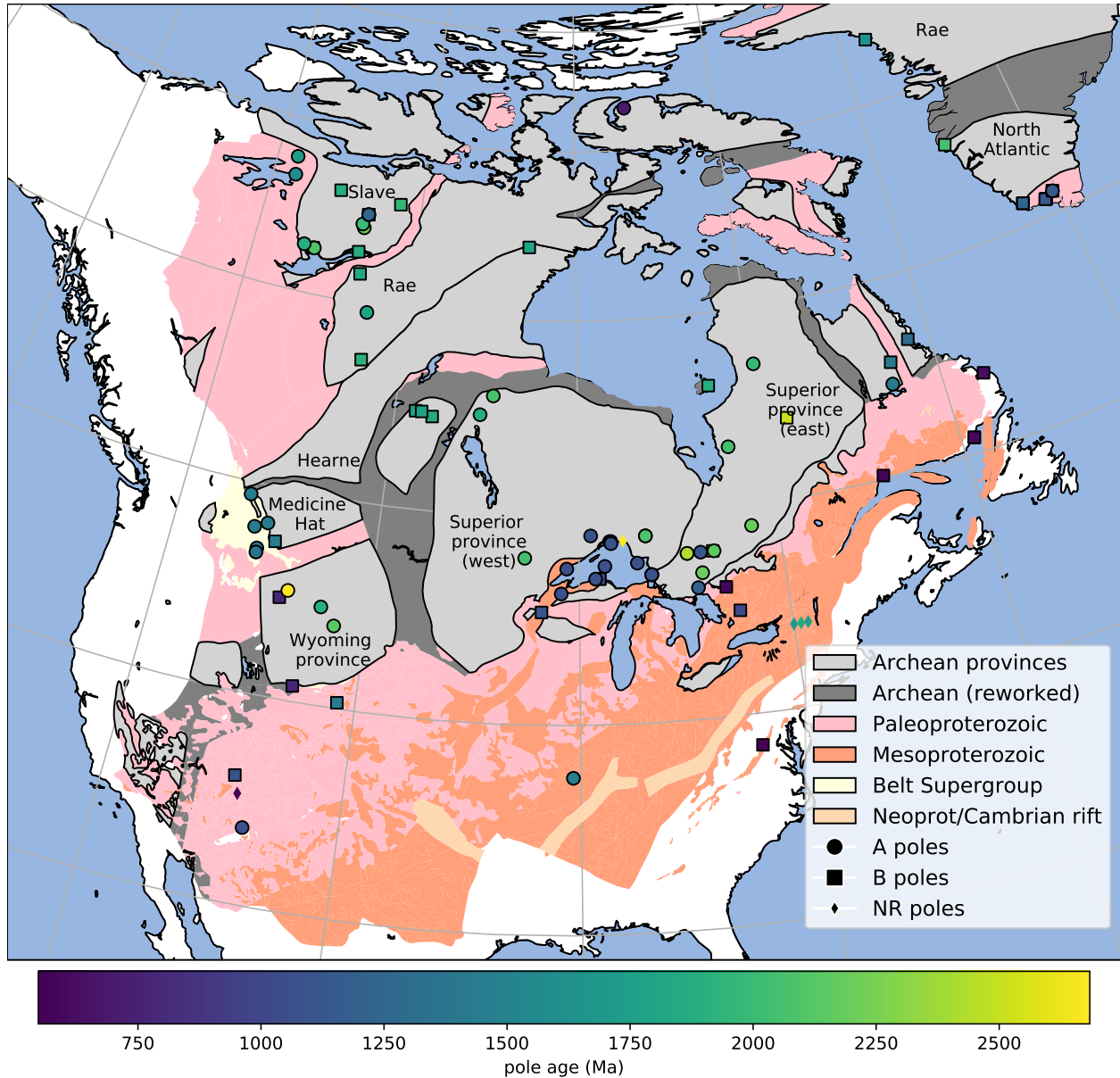


Figure 1. Simplified map of Laurentia showing the location of Archean provinces (labeled with text) and younger Paleoproterozoic and Mesoproterozoic crust (simplified from Whitmeyer and Karlstrom, 2007 with additions for Greenland based on St-Onge et al., 2009). The localities from which the compiled Precambrian paleomagnetic poles were developed are shown and colored by age. The circles (A rated poles) and squares (B rated poles) have been assessed by the Nordic workshop panel.

78 Canadian shield. Major growth of Laurentia following the amalgamation of these Archean
79 provinces occurred associated with the arc-continent collision of the ca. 1.71 to 1.68 Ga Yavapai
80 orogeny (Fig. 2). Yavapai orogenesis is interpreted to have resulted from the accretion of a series
81 of arc terranes that collided with each other and Laurentia (Karlstrom et al., 2001). Yavapai
82 accretion was followed by widespread emplacement of granitoid intrusions (Whitmeyer and
83 Karlstrom, 2007). These intrusions are hypothesized to have stabilized the juvenile accreted
84 terranes that subsequently remained part of Laurentia (Whitmeyer and Karlstrom, 2007).
85 Subsequent accretionary orogenesis of the ca. 1.65 to 1.60 Ga Mazatzal orogeny and associated
86 plutonism led to further crustal growth in the latest Paleoproterozoic (Karlstrom and Bowring,
87 1988). Laurentia's growth continued in the Mesoproterozoic along the southeast margin through
88 further juvenile terrane and arc accretion. An interval of major plutonism occurred ca. 1.48 to
89 1.35 Ga leading to the formation of A-type granitoids throughout both Mesoproterozoic and
90 Paleoproterozoic provinces extending from the southwest United States up to the Central Gneiss
91 Belt of Ontario to the northeast of Georgian Bay (Slagstad et al., 2009). This plutonism is likely
92 due to crustal melting within a back-arc region of ca. 1.50 to 1.43 Ga accretionary orogenesis
93 (Bickford et al., 2015). Geologic data from northern New Mexico have been interpreted to
94 indicate an interval of ca. 1.49 to 1.40 Ga orogenesis that has been named the Picuris orogeny
95 (Daniel et al., 2013). Younger magmatic activity ca. 1.37 Ga of the Southern Granite-Rhyolite
96 Province suggests a similar tectonic setting of accretionary orogenesis at that time (Bickford
97 et al., 2015). While an active margin interpretation with magmatism in a back-arc setting has
98 gained traction within the literature, the tectonic setting is often described as enigmatic given
99 earlier interpretations of an anorogenic setting (see references in Slagstad et al., 2009).

100 Accretionary orogenesis continued along the eastern margin of Laurentia with the
101 amalgamation and accretion of arcs associated with the ca. 1.25 to 1.22 Ga Elzevirian orogeny
102 (McLlland et al., 2013). The subsequent ca. 1.19 to 1.16 Ga Shawinigan orogeny is interpreted
103 to be due to the collision of terrane comprised of a previously rifted fragment of Laurentia and led
104 to obduction of the Pyrites Complex ophiolite (McLlland et al., 2010; Chiarenzelli et al., 2011).
105 The Shawinigan orogeny is followed by a period of tectonic quiescence on the eastern margin of
106 Laurentia until the collisional orogenesis of the Grenvillian orogeny (McLlland et al., 2010). An

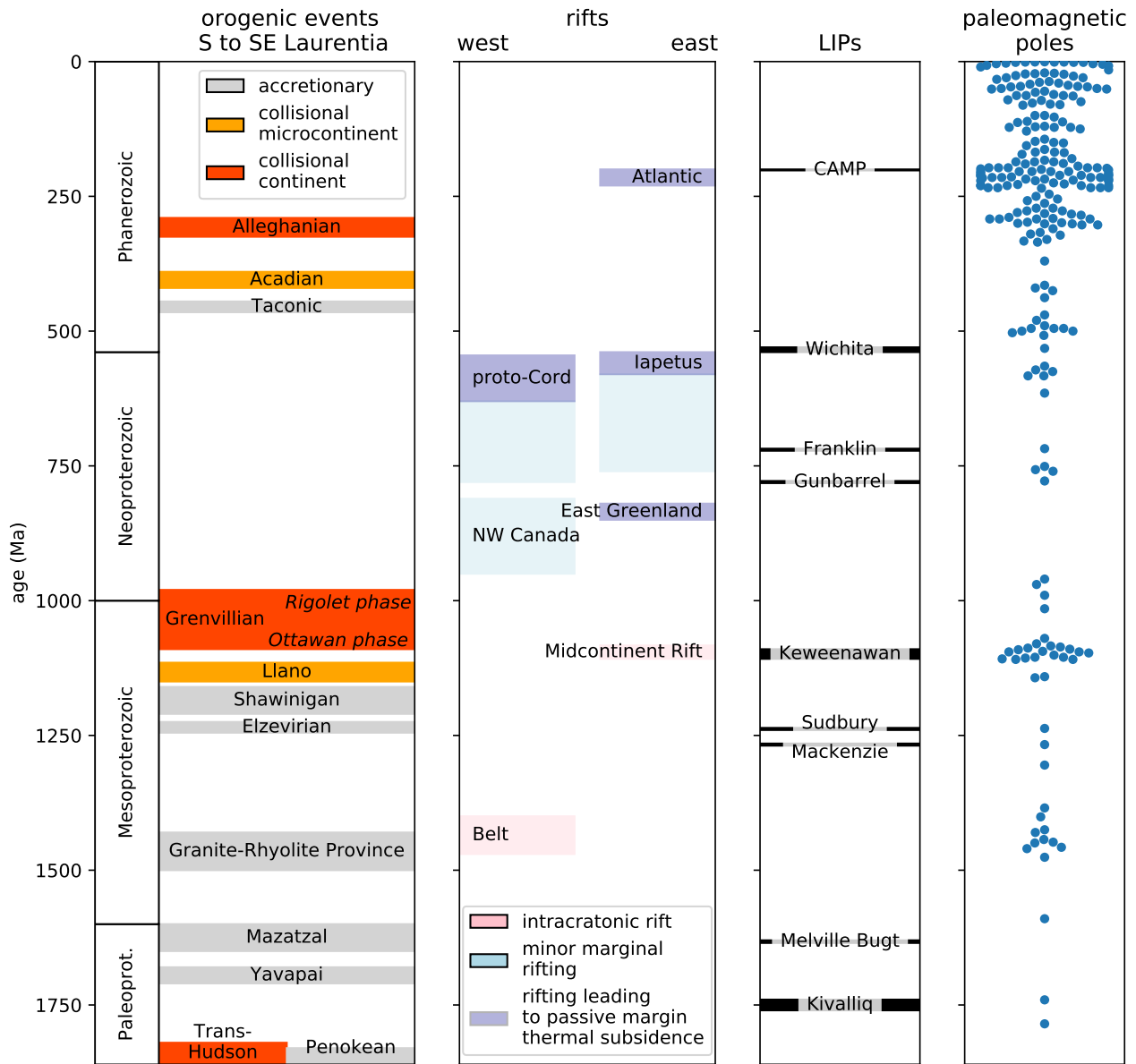


Figure 2. Simplified timeline of Laurentia's tectonic history over the past ~1.8 billion years. Brief summaries and references related to the orogenic and rifting episodes are given in the text. A timeline of large igneous provinces (LIPs) associated with typically brief and voluminous (or interpreted to be voluminous) volcanism is also shown. The interpreted age of paleomagnetic poles for Laurentia (not including separated terranes) compiled in this study for the Proterozoic and in Torsvik et al. (2012) for the Phanerozoic is shown. Abbreviations on the figure: CAMP (Central Atlantic Magmatic Province); proto-Cord (proto-Cordilleran).

107 exception to this quiescence during the interval between the Shawinigan and Grenvillian orogenies
108 is ca. 1.15 to 1.12 Ga orogenesis in the Llano uplift of the southern Laurentia margin (Mosher,
109 1998). Llano orogenesis is interpreted to have resulted from collision of continental lithosphere
110 along with an accreted arc (Mosher, 1998). This orogenesis is earlier and temporally distinct from
111 the Grenvillian orogeny, is only known from a limited spatial area, and is located in a region that
112 experienced further orogenesis during the Grenvillian orogeny (Grimes and Copeland, 2004).

113 Taken together, this context is suggestive of a microcontinent collision leading to Llano uplift
114 orogenesis prior to terminal Grenvillian continental collision. If this interpretation is correct, it is
115 similar to Paleozoic orogenesis along the margin where microcontinent collision resulted in the
116 Acadian orogeny prior to Alleghanian orogenesis during the Appalachian orogenic interval (2).

117 The Grenvillian orogeny was a protracted interval of continent-continent collision (ca. 1.09 to
118 0.98 Ga) leading to amphibolite to granulite facies metamorphism through the orogen (McLelland
119 et al., 2010). Evidence of large-scale continent-continent collision at the time of the Ottawan
120 Phase of the Grenvillian orogeny is recorded in Texas (Grimes and Copeland, 2004), up through
121 the Blue Ridge Appalachian inliers (Johnson et al., 2020), through Ontario and up to the
122 Labrador Sea (Rivers, 2008). The orogeny is interpreted to have resulted in the development of a
123 thick plateau associated with the Ottawan orogenic phase (ca. 1090 to 1030 Ma; Rivers, 2008).

124 Continued convergence during the Rigolet phase of the Grenvillian orogeny led to the
125 development of the Grenville Front tectonic zone and ended ca. 980 Ma (Hynes and Rivers, 2010).

126 In the latest Mesoproterozoic (ca. 1.11 to 1.08 Ga) prior to the Grenvillian orogeny, a major
127 intracontinental rift co-located with a large igneous province formed in Laurentia's interior
128 leading to extension within the Archean Superior province and adjacent Paleoproterozoic
129 provinces to the south (Cannon, 1992). This Midcontinent Rift led to the formation of a thick
130 succession of volcanics and mafic intrusions that are well-preserved in Laurentia's interior.
131 Midcontinent Rift development ceased as major collisional orogenesis of the Grenvillian orogeny
132 began (Swanson-Hysell et al., 2019).

133 There is significantly less preserved Mesoproterozoic crustal growth on the western margin of
134 Laurentia (Fig. 1), and the tectonic history through the Mesoproterozoic Era is not as well
135 elucidated as on the southern to eastern margin. The 15 to 20 km thick package of sedimentary

¹³⁶ rocks of the Belt-Purcell Supergroup is associated with a ca. 1.47 to 1.40 rift (Evans et al., 2000).
¹³⁷ While the rift is typically interpreted as being intracontinental (Lydon, 2004), the tectonic setting
¹³⁸ in which it formed is debated. Hoffman (1989) proposed that it may be a remnant back-arc basin
¹³⁹ trapped within a continent, while others envision it as being associated with continental rifting
¹⁴⁰ along the margin associated with separation of a conjugate continent (Jones et al., 2015). This
¹⁴¹ region is interpreted to have been subsequently deformed during a ca. 1.36 to 1.33 Ga event
¹⁴² known as the East Kootenay orogeny (McMechan and Price, 1982; Nesheim et al., 2012;
¹⁴³ McFarlane, 2015).

¹⁴⁴ This late Paleoproterozoic and Mesoproterozoic tectonic history provides significant
¹⁴⁵ constraints on paleogeographic reconstructions. In particular, the long-lived history of
¹⁴⁶ accretionary orogenesis along the southeast (present-day coordinates) of Laurentia from the
¹⁴⁷ initiation of the Yavapai orogeny (ca. 1.71 Ga) to the end of the Shawinigan orogeny (ca. 1.16
¹⁴⁸ Ga) requires a long-lived open margin without a major conjugate continent until the time of
¹⁴⁹ terminal Grenvillian orogeny collision (Karlstrom et al., 2001). This constraint is incorporated
¹⁵⁰ into models such as that of Zhang et al. (2012) and Pehrsson et al. (2015) which maintain a
¹⁵¹ long-lived convergent margin throughout the Mesoproterozoic, but in some reconstructions other
¹⁵² continental blocks are reconstructed into positions that are seemingly incompatible with this
¹⁵³ record of accretionary orogenesis (e.g. Amazonia in Elming et al., 2009). The high-grade
¹⁵⁴ metamorphism associated with the Ottawan phase of the Grenvillian orogeny itself strongly
¹⁵⁵ suggests a collision between Laurentia and (an)other continent(s) ca. 1080 Ma – the geological
¹⁵⁶ observation of which first led to the formulation of the hypothesis of the supercontinent Rodinia
¹⁵⁷ (Hoffman, 1991). This extensive and major collisional orogenic history recorded in Laurentia, and
¹⁵⁸ also present on other Proterozoic continents, at this time remains a strong piece of evidence that
¹⁵⁹ a supercontinent or (proto)supercontinent formed at the 1.0 Ga Mesoproterozoic to
¹⁶⁰ Neoproterozoic transition. Note that while the term Grenville orogeny or Grenville belt is used
¹⁶¹ rather loosely throughout much of the literature to refer to any late Mesoproterozoic orogenic
¹⁶² belt, the timeline of orogenesis on the Laurentia margin has more nuanced constraints than this
¹⁶³ usage. These constraints can be comparatively assessed when evaluating potential conjugate
¹⁶⁴ continents to Laurentia associated with the orogen (Fig. 2).

165 The subsequent Neoproterozoic tectonic history of Laurentia is dominantly a record of rifting
166 (Fig. 2). Along the western margin of Laurentia, rifting occurred ca. 780 to 720 Ma leading to
167 deposition in basins from the Death Valley region of SW Laurentia to the Mackenzie Mountains
168 of NW Laurentia (Macdonald et al., 2013; Dehler et al., 2017; Rooney et al., 2017). However, this
169 extensional basin development predates the rifting that led to well-documented passive margin
170 thermal subsidence closer to the ca. 539 Ma Neoproterozoic-Phanerozoic boundary (Bond et al.,
171 1984; Levy and Christie-Blick, 1991). The emplacement of the ca. 780 Ma Gunbarrel large
172 igneous province along this margin and the subsequent extension recorded in the basins is
173 commonly interpreted to be associated with the break-up of Laurentia and a conjugate continent
174 to the western margin (often interpreted to be Australia). If this interpretation is correct, it is
175 unclear why there would be minimal thermal subsidence until the Ediacaran (post 635 Ma as in
176 Levy and Christie-Blick, 1991 and Witkosky and Wernicke, 2018). The geological evidence
177 therefore supports prolonged active tectonism along the western margin of Laurentia (a portion of
178 which could be strike-slip and transtensional; Smith et al., 2015), but suggests that there was
179 significant lithospheric thinning associated with rifting later than the timing of rifting typically
180 implemented in models of Rodinia break-up. The record of Neoproterozoic basin development
181 lead Yonkee et al. (2014) to propose that the early ca. 780 Ma rifting was intracratonic and that
182 while it may have led to some associated thermal subsidence that there was a second interval of
183 rifting and thermal subsidence associated with Australia rifting away in the Ediacaran (later than
184 in most models). Another possibility, along the lines of that proposed in Ross (1991), is that ca.
185 780 Ma extensional tectonism is an inboard record of rifting and passive margin development that
186 occurred further outboard. In this model, subsequent continent rifting that drove lithospheric
187 thinning, perhaps associated with the departure of a microcontinent fragment rather than an
188 already departed major conjugate continent, would be the cause of Ediacaran to Cambrian
189 thermal subsidence.

190 In northwest Laurentia from the Ogilvie Mountains of Yukon to Victoria Island, the
191 sedimentary rock record is distinct from further south as it also records earlier Neoproterozoic
192 basin development during the Tonian Period in addition to Cryogenian basin development
193 (Macdonald et al., 2012). Tectonic extension is recorded in units of the lower Fifteenmile Group

194 with maximum depositional ages of ca. 1050 Ma with ongoing basin development ca. 812 Ma (age
195 constraint from a U-Pb zircon date on a tuff within the upper Fifteenmile Group; Macdonald
196 et al., 2010) potentially through thermal subsidence (Macdonald et al., 2012). Earlier basin
197 development in the region recorded by the Mesoproterozoic/Neoproterozoic Pinguicula Group
198 could provide valuable insight on tectonic history as it has been interpreted to have been
199 deposited in an extensional basin (Medig et al., 2016), however it is poorly constrained in terms of
200 age – older than the Fifteenmile Group and younger than the ca. 1382 Ma Hart River sills (which
201 themselves have been interpreted to be emplaced in conjunction with rifting; Verbaas et al., 2018).

202 Another margin that experienced rifting and associated passive margin thermal subsidence
203 earlier in the Neoproterozoic is the northeast Greenland margin (Fig. 2). Available
204 geochronological constraints and thermal subsidence modeling indicate ca. 850 to 820 Ma rifting
205 followed by thermal subsidence of a stable platform (Maloof et al., 2006; Halverson et al., 2018).
206 These data suggest that conjugate continental lithosphere had rifted away from northeast
207 Greenland by ca. 820 Ma.

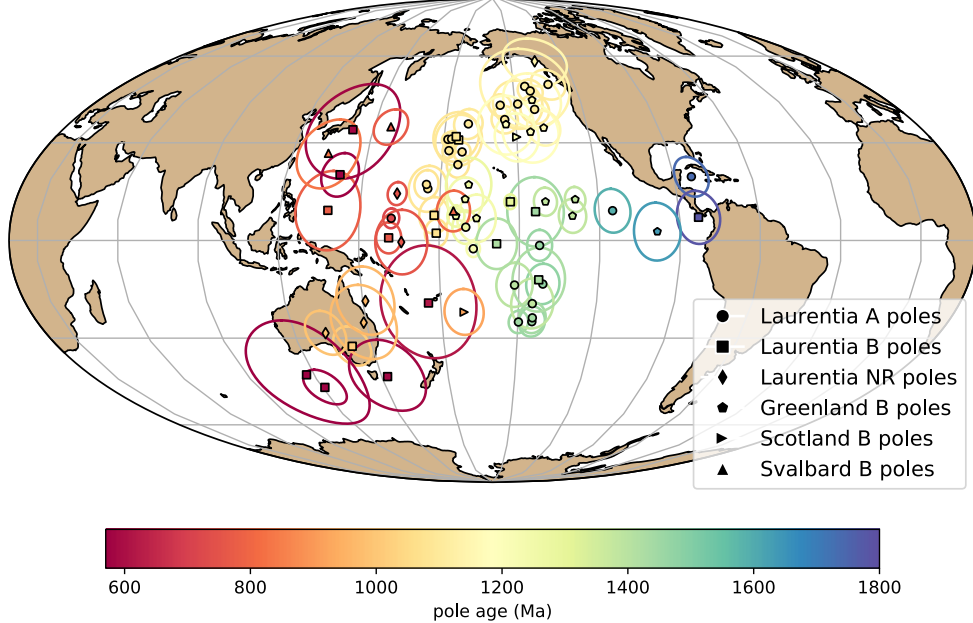
208 Extensive rifting followed by thermal subsidence occurred along the southeast to east Laurentia
209 margin in the time leading up to the Neoproterozoic-Phanerozoic boundary and is interpreted to
210 be associated with the opening of the Iapetus ocean. A record of this rifting is preserved as rift
211 basins that were part of failed arms (Rome trough, Reelfoot rift and Oklahoma aulacogen; Fig. 1)
212 as well as prolonged Cambrian to Ordovician passive margin thermal subsidence along the margin
213 (Bond et al., 1984; Whitmeyer and Karlstrom, 2007). The age of igneous intrusions that have
214 been interpreted to be rift-related play a significant role in interpretations of this history such as
215 in the rift development model of Burton and Southworth (2010). In this model,
216 spatially-restricted rifting occurs ca. 760 to 680 Ma in the region of modern-day North Carolina
217 and Virginia. Rifting ca. 620 to 580 Ma initiates in the region from modern-day New York to
218 Newfoundland and by ca. 580 to 550 Ma rifting extends along the length of Laurentia's eastern
219 margin. The last phase of this rifting has been interpreted to be associated with the separation of
220 the Argentine pre-Cordillera Cuyania terrane (Dickerson and Keller, 1998). As with other rifts, it
221 is difficult to distinguish the separation of a cratonic fragment as a microcontinent from the
222 rifting and departure of a major craton, as the record that lingers on the craton is similar.

223 Recognizing this ambiguity, Robert et al. (2020) propose that rather than being associated with
224 spatially-restricted or failed rifting that ca. 700 Ma extension is associated with breakup and
225 separation of Laurentia and its conjugate continent (that they interpret to be Amazonia). This
226 rifting would have led to the formation of the Paleo-Iapetus Ocean (an analogue with the
227 Paleo-Tethys). Subsequent to this rifting of the major continental blocks, smaller terranes of
228 lithosphere rift off the east Laurentia ca. 600 Ma leading to the formation of the Neo-Iapetus
229 Ocean and the record of passive margin development on Laurentia (Robert et al., 2020).

230 The eastern margin of Laurentia then went through the multiple phases of Appalachian
231 orogenesis. As is visualized in Figure 2, there are parallels between the Grenville orogenic interval
232 and the Appalachian orogenic interval in that there was a period of arc-continent collision
233 (Elzevirian orogeny in the Grenville interval; Taconic orogeny in the Appalachian interval)
234 followed by microcontinent accretion (Shawinigan/Llano orogenies in the Grenville interval;
235 Acadian orogeny in the Appalachian interval) that culminated in large-scale continent-continent
236 collision (Grenvillian orogeny in the Grenville interval; Alleghanian orogeny in the Appalachian
237 interval). These similarities are the consequence of an active margin facing an ocean basin that
238 was progressively consumed until continent-continent collision. In the case of the Grenville
239 interval, this terminal collision is interpreted to be associated with the assembly of the
240 supercontinent Rodinia, and in the Appalachian interval it is interpreted to be associated with
241 the assembly of the supercontinent Pangea.

242 Even without considering other continents on Earth, the geological record of Paleoproterozoic
243 collisional of Archean provinces combined with accretionary orogenesis at that time and through
244 the rest of the Paleoproterozoic and Mesoproterozoic Eras provides strong evidence for mobile
245 plate tectonics driving Laurentia's evolution throughout the past 2 billion years. This tectonic
246 history inferred from geological data can be enhanced through integration with the paleomagnetic
247 record.

Poles for Laurentia (post-Paleoproterozoic amalgamation; with terranes)



Poles for Laurentia (pre-Paleoproterozoic amalgamation)

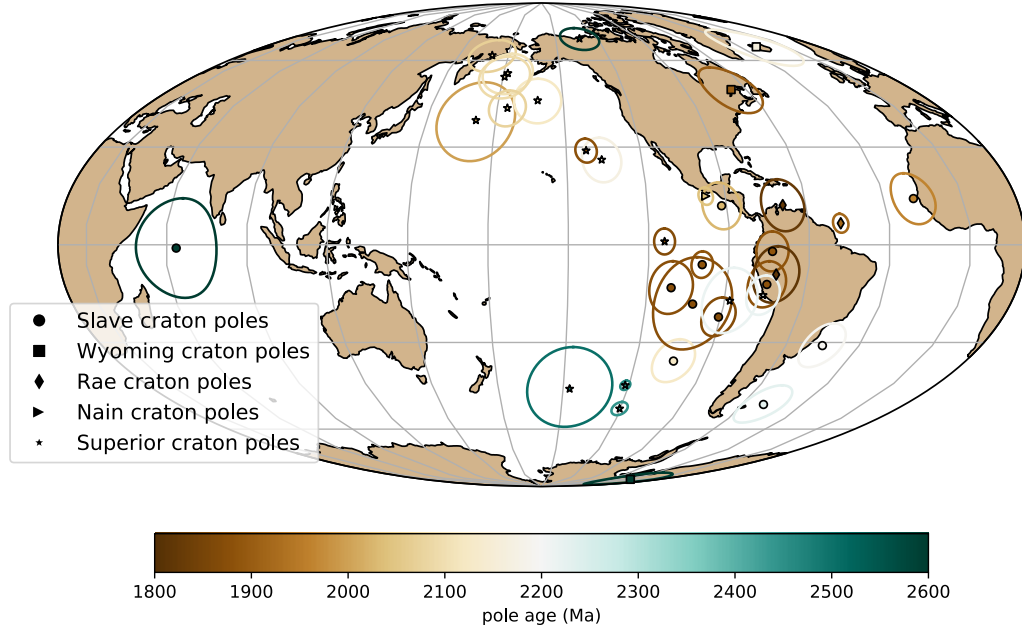


Figure 3. Top panel: Paleomagnetic poles from 1800 to 560 Ma for Laurentia (including Greenland, Scotland and Svalbard). Bottom panel: Paleomagnetic data for Archean Provinces prior to the amalgamation of Laurentia.

²⁴⁸ **4.3 Paleomagnetic pole compilation**

²⁴⁹ In this chapter, I focus on the compilation of paleomagnetic poles developed through the Nordic
²⁵⁰ Paleomagnetism Workshops with some additions and modifications (Fig. 3 and Table 2). The
²⁵¹ Nordic Paleomagnetism Workshops have taken the approach of using expert panels to assess
²⁵² paleomagnetic poles and assign them grades meant to convey the confidence that the community
²⁵³ has in these results (Evans et al., this volume). While many factors associated with
²⁵⁴ paleomagnetic poles can be assessed quantitatively through Fisher statistics and the precision of
²⁵⁵ geochronological constraints, other aspects such as the degree to which available field tests
²⁵⁶ constrain the magnetization to be primary require expert assessment. The categorizations used by
²⁵⁷ the expert panel are ‘A’ and ‘B’ with the last panel meeting occurring in Fall 2017 in Leirubakki,
²⁵⁸ Iceland. The ‘A’ rating refers to poles that are judged to be of such high quality that they
²⁵⁹ provide essential constraints that should be satisfied in paleogeographic reconstructions. The ‘B’
²⁶⁰ rating is associated with poles that are judged to likely provide a high-quality constraint, but
²⁶¹ have some deficiency such as remaining ambiguity in the demonstration of primary remanence or
²⁶² the quality/precision of available geochronologic constraints. Additional poles that were not given
²⁶³ an ‘A’ or ‘B’ classification at the Nordic Workshops are referred to as not-rated (‘NR’). These
²⁶⁴ additional poles are taken from the Paleomagia database (Veikkolainen et al., 2014). Many of
²⁶⁵ these poles in the Paleomagia database are quite valuable for reconstruction and should not be
²⁶⁶ dismissed from being considered in paleogeographic reconstructions. However, there are
²⁶⁷ ambiguities associated with many of the poles not given Nordic ‘A’ or ‘B’ ratings in terms of how
²⁶⁸ well the nature of the remanence is constrained, including its age. For example, there are rich
²⁶⁹ data associated with intrusive and metamorphic lithologies of the Grenville Province that are the
²⁷⁰ available paleomagnetic constraints for Laurentia at the Mesoproterozoic-Neoproterozoic
²⁷¹ boundary. However, the ages of the remanence associated with these poles is complicated by the
²⁷² reality that the magnetization was acquired during exhumation and such cooling ages are more
²⁷³ difficult to robustly constrain than the ages of remanence associated with dated eruptive units or
²⁷⁴ shallow-level intrusions. As a result, the vast majority of Grenville Province poles are not given
²⁷⁵ an ‘A’ or ‘B’ rating with the exception of the ‘B’ rated pole from the ca. 1015 Ma Haliburton
²⁷⁶ intrusions. However, while any one of these Grenville poles could be interpreted to suffer from

277 large temporal uncertainty, the overall preponderance of poles in a similar location at the time
278 suggests that they need to be taken seriously within paleogeographic reconstructions of Laurentia
279 (although an alternative view of an allochthonous origin put forward by Halls et al. (2015) is
280 discussed below). In this compilation, the poles of Brown and McEnroe (2012) from the
281 Adirondack highlands are used wherein the magnetic mineralogy and associated relative ages of
282 remanence are relatively well-constrained (Table 2). An additional not-rated pole included in the
283 present compilation is the new pole for the ca. 1144 Ma Ontario lamprophyre dikes (Piispa et al.,
284 2018) that strengthens the position of Laurentia at the time and coincides with the position of the
285 poles from the ca. 1140 Ma Abitibi dikes (Ernst and Buchan, 1993). This pole will likely receive
286 an ‘A’ rating when assessed at the next Nordic paleomagnetism workshop. Poles from the
287 Neoproterozoic Chuar Group of southerwest Laurentia as presented in Eyster et al. (2019) are
288 also included.

289 **4.4 Differential motion before Laurentia amalgamation**

290 Prior to the termination of the Trans-Hudson orogeny (before 1.8 Ga), paleomagnetic poles need
291 to be considered with respect to the individual Archean provinces. For the Superior province, an
292 additional complexity is that paleomagnetic poles from Siderian to Rhyacian Period (2.50 to 2.05
293 Ga) dike swarms, as well as deflection of dike trends, support an interpretation that there was
294 substantial Paleoproterozoic rotation of the western Superior province relative to the eastern
295 Superior province across the Kapuskasing Structural Zone (Bates and Halls, 1991; Evans and
296 Halls, 2010). This interpretation is consistent with the hypothesis of Hoffman (1988) that the
297 Kapuskasing Structural Zone represents major intracratonic uplift related to the Trans-Hudson
298 orogeny. Evans and Halls (2010) propose an Euler rotation of (51°N, 85°W, -14°CCW) to
299 reconstruct western Superior relative to eastern Superior and interpret that the rotation occurred
300 in the time interval of 2.07 to 1.87 Ga. I follow this interpretation and group the poles into
301 Superior (West) and Superior (East). Uncertainty remains with respect to whether the ca. 1.88
302 Ga Molson dikes pole pre-dates or post-dates this rotation (Evans and Halls, 2010) and thus for
303 the time being should be considered solely in the western Superior province reference frame.

304 There are poles in the compilation for the Slave, Wyoming, Rae, Superior and North Atlantic

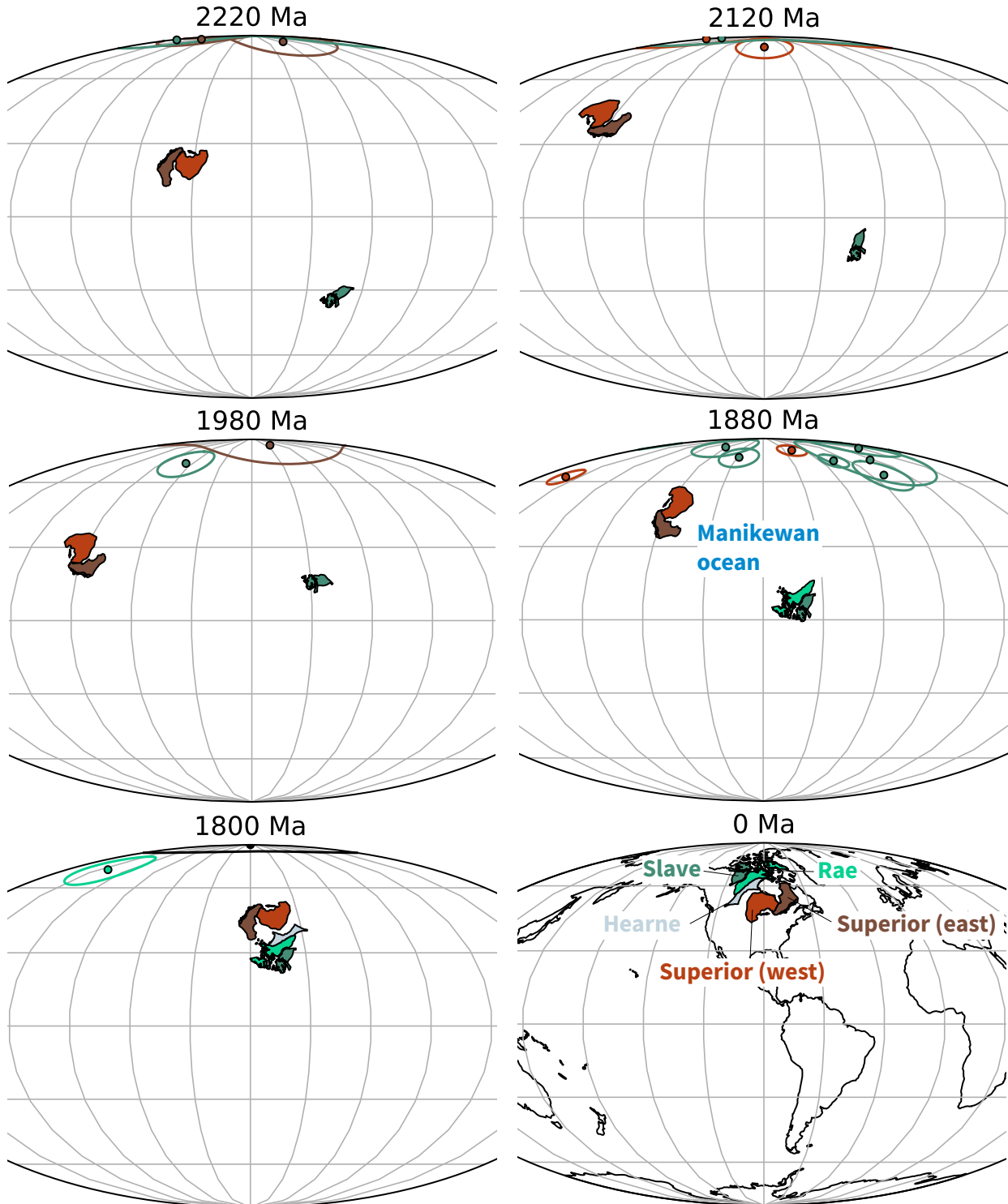


Figure 4. Paleogeographic reconstructions developed using poles from the Superior, Slave and Rae provinces. The polarity options that are chosen for the provinces are those that minimize total apparent polar wander path length. This model reconstructs a wide Manikewan ocean that underwent orthogonal closure rather than an alternative possibility of narrower Manikewan with a pivot-like closure. Paleomagnetic poles are shown colored to match their respective province with these provinces shown in present-day coordinates and labeled in the 0 Ma panel. Poles with ages that are within 25 million years of the given time slice are shown. The relatively well-resolved pole paths from the Superior and Slave provinces (Fig. 3) that are utilized for these reconstructions provide strong support for differential plate tectonic motion between 2220 and 1850 Ma.

provinces prior to Laurentia amalgamation (Fig. 3 and Table 2). Overall, these data provide an opportunity to re-evaluate the paleomagnetic evidence for relative motions between Archean provinces prior to Laurentia assembly. A lingering question raised in Hoffman (1988) is to what extent the Archean provinces each had independent drift histories with significant separation or shared histories before experiencing fragmentation and reamalgamation. The strongest analysis in this regard comes from comparisons between paleomagnetic poles between the Superior and Slave provinces (Buchan et al., 2009; Mitchell et al., 2014; Buchan et al., 2016). High-quality paleomagnetic poles from these two provinces provide strong support for differential motion between the Superior and Slave provinces between 2.2 and 1.8 Ga with the two provinces not being in their modern-day relative orientation to one another and having distinct pole paths as constrained by five time slices of nearly coeval poles from 2.23 and 1.89 Ga (Fig. 4; Buchan et al., 2016). These data provide paleomagnetic support for the Superior and Slave provinces having independent histories of differential motion. The data also support the hypothesis that the Trans-Hudson orogeny is the result of terminal collision associated with the closure of an ocean basin between the Superior province and the Hearne+Rae+Slave provinces. Reconstructions developed for this chapter of the Superior and Slave provinces using these poles are shown in Figure 4 and illustrate the difference in implied orientation and paleolatitude that results from these well-constrained poles.

4.5 Paleogeography of an assembled Laurentia

Following the amalgamation of the Archean provinces in Laurentia ca. 1.8 Ga, poles from each part of Laurentia can be considered to reflect the position of the entire composite craton. It is worth considering the possibility that poles from zones of Paleoproterozoic and Mesoproterozoic accretion could be allochthonous to the craton. Halls (2015) argued that this was the case for late Mesoproterozoic and early Neoproterozoic poles from east of the Grenvillian allochthon boundary fault. However, the majority of researchers have considered these poles to post-date major differential motion and be associated with cooling during collapse of a thick orogenic plateau developed during continent-continent collision (e.g. Brown and McEnroe, 2012). Poles with a B-rating are also included in the compilation that come from Greenland, Svalbard and Scotland.

333 These terranes were once part of contiguous Laurentia, but have subsequently rifted away. These
334 poles need to be rotated into the Laurentia reference frame prior to use for tectonic
335 reconstruction, and I apply the rotations shown in Table 1. The Euler pole and rotation is quite
336 well-constrained for Greenland as it is associated with recent opening of Baffin Bay and the
337 Labrador Sea (for which the rotation of Roest and Srivastava, 1989 is used). The reconstruction
338 of Scotland is associated with the opening of the Atlantic (for which the rotation employed by
339 Torsvik and Cocks, 2017 is used) which is well-constrained, but has more uncertainty associated
340 with the Euler pole than that for Greenland. The reconstruction of Svalbard is more challenging
341 given a multi-stage tectonic history involving both translation within the Caledonides and
342 subsequent rifting. The preferred Euler pole parameters of Maloof et al. (2006) are used here for
343 this reconstruction. This Euler rotation is designed, in particular, to honor the high degree of
344 similarity between Tonian sediments in East Greenland (Hoffman et al., 2012) and those of East
345 Svalbard (Maloof et al., 2006) and to reconstruct East Svalbard to be aligned with these
346 correlative sedimentary rocks.

347 Through the Proterozoic, there are intervals where there are abundant paleomagnetic poles
348 that constrain Laurentia's position and intervals when the record is sparse (shown colored by age
349 in Fig. 3). To further visualize the temporal coverage of the poles and to summarize the motion,
350 implied paleolatitudes for an interior point on Laurentia are shown in Figure 5. The ages of the
351 utilized paleomagnetic poles are also shown in comparison to the simplified summary of tectonic
352 events in Figure 2. Both collisional and extensional tectonism can result in the formation of
353 lithologies that can be used to develop paleomagnetic poles either as a result of basin formation,
354 magmatism or both. In addition, intraplate magmatism resulting from plume-related
355 large-igneous provinces can lead to paleomagnetic poles in periods that are otherwise
356 characterized by tectonic quiescence (e.g. the ca. 1267 Ma Mackenzie LIP; Fig. 2).
357 Intracontinental rifts have led to the highest density of poles both in the case of the ca. 1.4 Ga
358 Belt Supergroup and the ca. 1.1 Ga Midcontinent Rift (Fig. 2). The quality and resolution of the
359 record from the Midcontinent Rift is aided by the voluminous magmatism that occurred in
360 conjunction with basin formation that enables the development of a well-calibrated apparent
361 polar wander path (Swanson-Hysell et al., 2019). The late Tonian Period also has a number of

362 poles including the Gunbarrel LIP (ca. 780 Ma) and Franklin LIP (ca. 720 Ma), as well as
363 similarly-aged sedimentary rocks from western Laurentia basins (Eyster et al., 2019). Overall,
364 there is internal consistency among the paleomagnetic poles within intervals for which there is
365 high-resolution coverage. These data result in progressive paths such as ascending up to the
366 Logan Loop, down the Keweenawan Track (Swanson-Hysell et al., 2019) to the Grenville Loop
367 prior to a temporal gap before the late Tonian (ca. 775 to 720 Ma) path (Eyster et al., 2019).

368 Data from other terranes add resolution to the record. In particular, data from Greenland add
369 12 poles between 1385 and 1160 Ma when there are only four poles from mainland Laurentia.
370 Given that the rotation between Greenland and mainland Laurentia is well-constrained (Table 1),
371 once rotated these poles can be used for reconstruction of the entire continent. The reliability of
372 this approach gains credence through the good agreement between the ca. 1633 Ma Melville Bugt
373 diabase dikes pole from Greenland (Halls et al., 2011) and the ca. 1590 Ma Western Channel
374 diabase pole of mainland Laurentia (Irving and Park, 1972). Similarly, there is good agreement
375 between the ca. 1267 Ma Mackenzie dikes pole of Laurentia (Buchan et al., 2000) and coeval
376 poles from Greenland such as the ca. 1275 Ma North Qoroq intrusives (Piper, 1992) and Kungnat
377 Ring dike (Piper, 1977). Furthermore, the Greenland poles with ages that fall between the ca.
378 1237 Ma Sudbury dikes and ca. 1144 Ma lamprophyre dikes pole of mainland Laurentia are
379 consistent with constraints on either side from the mainland while filling in the ascending limb of
380 the path leading up to the apex of 1140 to 1108 Ma poles known as the Logan Loop.

381 An exception to this overall agreement between poles from Greenland and mainland Laurentia
382 occurs ca. 1382 Ma. There are poles of this age from Greenland associated with the Zig-Zag Dal
383 basalts and related intrusions (Marcussen and Abrahamsen, 1983; Abrahamsen and Van Der Voo,
384 1987). However, these poles are in a distinct location from poles of similar age associated with the
385 Belt Supergroup (e.g. the McNamara Formation and Pilcher/Garnet Range and Libby
386 Formations; Elston et al., 2002). Additionally, the older Belt Supergroup poles form a more
387 southerly population than time-equivalent poles from elsewhere in Laurentia such as the Mistastin
388 Pluton. There are potential complications associated with the Belt Supergroup being exposed
389 within thrust sheets with significant Cenozoic Mesozoic and Cenozoic deformation. However,
390 vertical axis rotations of the Belt region are not able to bring the Belt poles into agreement with

391 those from Laurentia or Greenland nor is translation away from the craton. Another potential
392 complication is that the remanence used for the development of the Belt Supergroup resides in
393 hematite. As a result, there is the potential for inclination-flattening within the sedimentary rocks
394 from which poles are developed. However, applying a moderate inclination factor of $f = 0.6$ also
395 does not bring the poles into congruence with the Zig-Zag basalts. There is the potential that the
396 hematite could be the result of post-depositional oxidation (the remanence of the lavas pole is
397 also held by hematite), however the overall coherency of the pole directions and the presence of
398 reversals has been taken as evidence that the remanence is primary (Elston et al., 2002). At
399 present, it is unclear which poles are a better representation of Laurentia's position ca. 1400 Ma.

400 Another challenging portion of the Laurentia paleomagnetic record is that for the Ediacaran
401 Period where there are inconsistencies between poles of similar age (Figs. 3 and 5). As a result,
402 there are poles that imply both low-latitude and high-latitude positions of Laurentia between 583
403 and 565 Ma (Fig. 5). This conflicting record is a longstanding problem and has led to the
404 presentation of both high-latitude and low-latitude Laurentia paleogeographic reconstructions at
405 the time (e.g. Pisarevsky et al., 2001; Li et al., 2008). One explanation for these variable pole
406 positions is that they are the result of large-scale oscillatory true polar wander in the Ediacaran
407 where rapid rotation of the entire silicate Earth influenced poles in Baltica and West Africa as
408 well (McCausland et al., 2007; Robert et al., 2017). Paleodirectional data from single feldspar
409 crystals from the Sept-Îles layered intrusion led Bono and Tarduno (2015) to interpret the lower
410 inclination (and therefore lower latitude) direction from the intrusion (the one included as the
411 Sept-Îles pole in Table 2; Tanczyk et al., 1987) as the primary thermal remanent magnetization
412 and that interpret steeper directions also recovered from the intrusives as the result of
413 remagnetization. They suggest that other steep magnetizations from Ediacaran Laurentia
414 plutonic rocks, such as that observed in the ca. 583 Ma Baie des Mountons complex (the A group
415 of McCausland et al. (2011) in Table 2), are also the result of remagnetization. Notably the lower
416 inclination Baie des Mountons complex B Group directions result in a pole that is
417 indistinguishable from the lower inclination Sept-Îles intrusives pole. Another possibility
418 discussed in the literature is that the lack of congruency between poles in this time interval is due
419 to a particularly weak and non-dipolar geomagnetic field (Abrajevitch and Van der Voo, 2010;

⁴²⁰ Halls et al., 2015; Bono et al., 2019). Data from the ca. 585 Ma Grenville dyke swarm interpreted
⁴²¹ as primary reveal $\sim 90^\circ$ differences in direction within dikes dated within to high-precision 4
⁴²² million years of one another (Halls et al., 2015). The rates of $>20^\circ/\text{Myr}$ ($>220 \text{ cm/yr}$) implied if
⁴²³ these data are interpreted as resulting from plate motion or true polar wander were considered as
⁴²⁴ dynamically implausible by Halls et al. (2015) leading the authors to favor a deviation from axial
⁴²⁵ dipolar behavior as the explanation for disparate Ediacaran directions. Regardless of mechanism,
⁴²⁶ the Ediacaran data stand out as anomalous relative to the coherency of the rest of the poles in
⁴²⁷ the composite (Fig. 5).

⁴²⁸ Synthesizing the compilation of paleomagnetic poles for Laurentia into a composite path over
⁴²⁹ the past 1.8 billion years presents a challenge given the highly variable temporal coverage. The
⁴³⁰ method typically applied in the Phanerozoic is to develop synthesized pole paths either through
⁴³¹ fitting spherical splines through the data or calculating binned running means where the Fisher
⁴³² mean of poles within a given interval are calculated (Torsvik et al., 2012). Applying such an
⁴³³ approach can reduce the influence of spurious poles. Such synthesis is particularly important in
⁴³⁴ regions of high data density where seeking to satisfy every mean pole position would result in
⁴³⁵ jerky motion.

⁴³⁶ A synthesized pole path for Laurentia is developed here and used to develop a paleogeographic
⁴³⁷ reconstruction of Laurentia constrained by the compilation of paleomagnetic poles. The
⁴³⁸ paleolatitude implied by this continuous model is shown in Figure 5. This path is based on
⁴³⁹ Laurentia data alone which means that it is poorly constrained through intervals of sparse data
⁴⁴⁰ (950-850 Ma for example). One could use interpretations of paleogeographic connections with
⁴⁴¹ other cratons (e.g. Baltica in the early Neoproterozoic) to fill in such portions of the path,
⁴⁴² however the result then becomes model-dependent without being constrained by data from
⁴⁴³ Laurentia itself. In portions of the record with a more dense record of poles, such as ca. 1450 Ma,
⁴⁴⁴ a calculated running mean is used to integrate constraints from multiple poles. This method
⁴⁴⁵ follows the approach taken in the Phanerozoic (e.g. Torsvik et al., 2012 wherein all poles within a
⁴⁴⁶ 20 Myr interval are averaged with the interval than progressively moved forward in 10 Myr steps.
⁴⁴⁷ When there are isolated ‘A’ grade poles without other temporally-similar poles, these poles are
⁴⁴⁸ fully satisfied in model. Where there are no constraints a simple interpolation between constraints

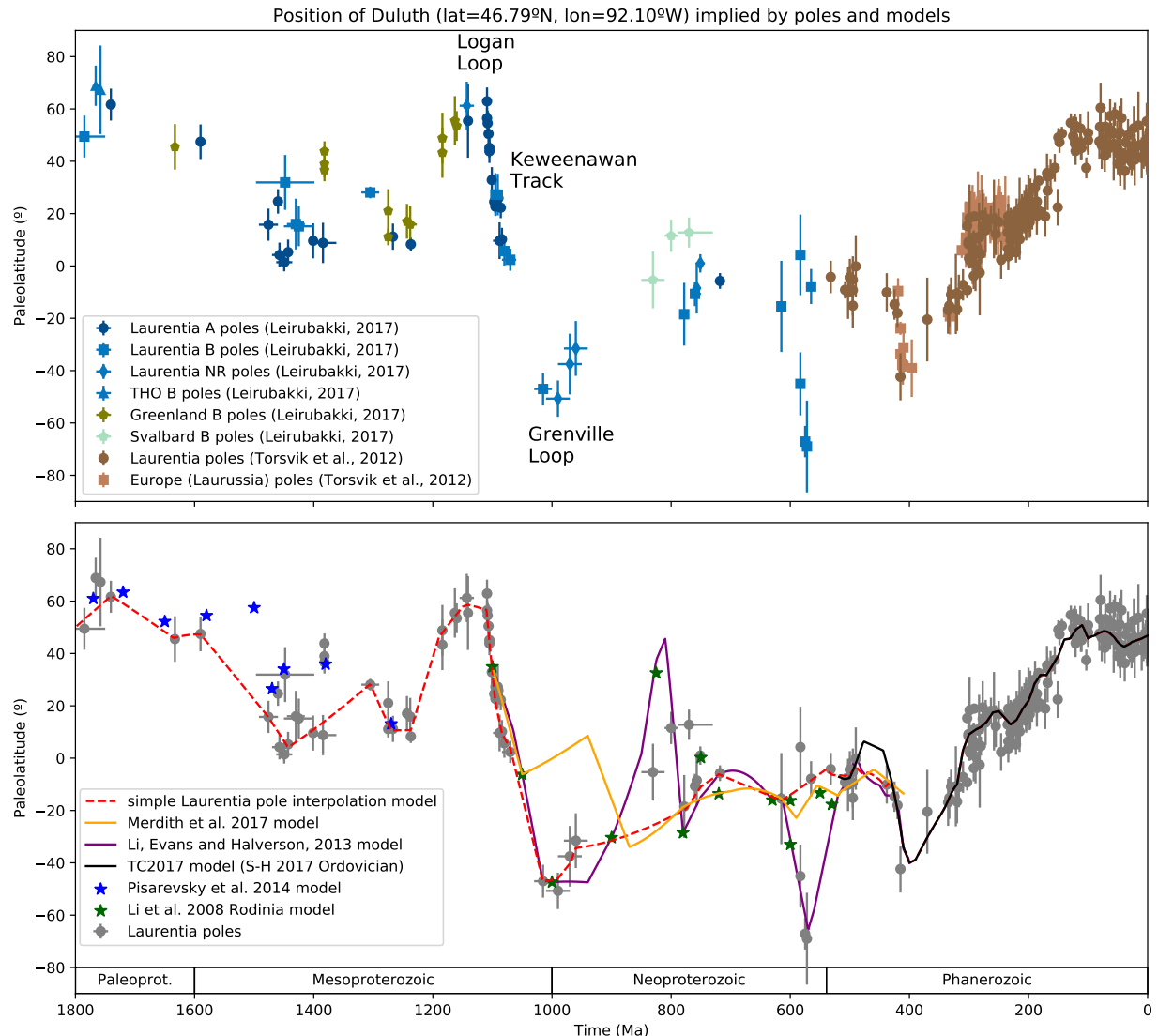


Figure 5. Top panel: Paleolatitude implied by paleomagnetic poles from Laurentia and associated blocks for Duluth (lat= 46.79° N, lon= 92.10° W). The paleomagnetic poles are compiled in Table 2. Bottom panel: Paleolatitude implied by Laurentia poles compared with that implied by published paleogeographic models and the simple Laurentia model used in this chapter for the reconstructions in Figure 7.

449 is made. While data from Scotland and Svalbard are associated with Laurentia, the Scotland
450 poles are poorly constrained in time and the Svalbard rotation to Laurentia is uncertain. These
451 poles are not utilized in the simple Laurentia model which means that the model as shown does
452 not include oscillatory true polar wander interpreted to have occurred ca. 810 and 790 Ma based
453 on data from Svalbard (Maloof et al., 2006). The model of Li et al. (2013) shown in Figure 5 does
454 seek to incorporate this true polar wander while also incorporating an interpretation of the
455 paleomagnetic pole record from South China.

456 One downside of a running mean approach is that it pulls the mean to regions of high data
457 density. As was shown in Swanson-Hysell et al. (2019), this behavior can reduce motion along an
458 apparent polar wander path. As a result, for the portion of the reconstruction during the interval
459 of time ca. 1110 to 1070 Ma where there is high data density from the Midcontinent Rift, I utilize
460 an Euler pole inversion from Swanson-Hysell et al. (2019).

461 Paleogeographic snapshots for the past position of Laurentia reconstructed using this synthesis
462 of the paleomagnetic poles are shown in Figure 7. These reconstructions use the tectonic elements
463 as defined by Whitmeyer and Karlstrom (2007) with these elements being progressively added
464 associated with Laurentia's accretionary growth. As a reminder to the reader, paleomagnetic
465 poles provide constraints on the paleolatitude of a continental block as well as its orientation
466 (which way was north relative to the block). While they provide constraints in this regard, they
467 do not provide constraints in and of themselves for the longitudinal position of the block. Other
468 approaches to obtain paleolongitude utilize geophysical hypotheses such as assuming that large
469 low shear velocity provinces have been stable plume-generating zones in the lower mantle to
470 which plumes can be reconstructed (Torsvik et al., 2014) or that significant pole motion in certain
471 time intervals is associated with true polar wander axes with specified paleolongitudes that switch
472 through time in conjunction with the supercontinent cycle (Mitchell et al., 2012). In Figure 7,
473 Laurentia is centered on the longitudinal position of Duluth with the orientation and
474 paleolatitude being constrained by the paleomagnetic pole compilation as synthesized in the
475 simple Laurentia pole interpolation model (Fig. 5).

476 **4.6 Paleoenvironmental constraints on paleolatitude**

477 Sedimentary rocks whose deposition is associated with specific climatic conditions have the
478 potential to provide insight into paleolatitude. Relevant deposits in the Proterozoic include glacial
479 deposits deposited by continental ice sheets, carbonates deposited in carbonate-saturated (and
480 thereby likely to be warm) marine environments, and evaporite deposits deposited where
481 evaporation exceeded precipitation. Interpretations of paleolatitude based on glacial deposits are
482 complicated by the evidence for multiple global and low-latitude glacial intervals during the
483 Proterozoic (Evans and Heller, 2003). Evaporite deposits are particularly compelling as
484 paleolatitude constraints given that their deposition is interpreted to be associated with arid
485 regions resulting from large-scale Hadley cell downwelling (Evans, 2006). While moisture in the
486 subtropics can change along with Earth's climate, the overall pattern of $\sim 10\text{--}35^\circ$ of latitude being
487 where annual mean evaporation exceeds precipitation persists (Burls and Fedorov, 2017). Using a
488 compilation of paired paleomagnetically-determined paleolatitude constraints and evaporite
489 occurrence, Evans (2006) demonstrated that over the past 2 Ga large-scale evaporite deposition
490 was consistently located in subtropical latitudes that correspond to modern arid zones. This
491 finding is consistent both with the geocentric axial dipole hypothesis used to calculate
492 paleolatitude and the long-term stability of large-scale convection circulation cells.

493 There is high evaporation in the subtropics and tropics. Within the tropical rain belt (0 to
494 $\sim 10^\circ$ latitude) these high evaporation rates are typically overwhelmed by precipitation such that
495 global zonal mean precipitation exceeds evaporation within $\sim 10^\circ$ of the equator (within $\sim 8^\circ$ of
496 the equator over land) with evaporation exceeding precipitation from those latitudes towards
497 higher ones with evaporation minus precipitation being at a maximum at $\sim 20\text{--}25^\circ$. However,
498 continental interiors near the equator can also be arid due to regional precipitation patterns
499 leading to the precipitation of evaporites. For example, Lake Magadi in Kenya at a latitude of
500 1.9° S is a saline lake where thick bedded evaporites have accumulated (Eugster, 1980). Caution is
501 therefore needed when interpreting paleolatitude from evaporites in terrestrial and intracratonic
502 settings given that they could occur both in tropical and subtropical latitudes.

503 Proterozoic evaporite deposits are documented within these units that were deposited

504 following the amalgamation of Laurentia:

- 505 • The Altyn Formation of the Belt Supergroup contains pseudomorphs after gypsum crystals
506 and anhydrite within shallow-water carbonates with relict gypsum and anhydrite
507 preserved within secondary silica (White, 1984). The correlative Prichard Formation is
508 intruded by 1468.8 ± 2.5 Ma sills (Sears et al., 1998). Halite molds and casts are present
509 within mudstones of the overlying Grinell Formation (Pratt and Ponce, 2019). Higher in the
510 Belt Supergroup stratigraphy, within the Wallace Formation, there is stratiform scapolite —
511 a metamorphic mineral interpreted to have formed from a halite precursor within the
512 Wallace Formation (Hietanen, 1967). There are also halite and gypsum pseudomorphs
513 within carbonate mudstones of the correlative to underlying Helena Formation (Pratt, 2001;
514 WINSTON, 2007). These deposits are older than the 1443 ± 7 Ma Purcell lavas and further
515 constrained in age by a tuff with a U-Pb date of 1454 ± 9 within the Helena Formation
516 (Evans et al., 2000).
- 517 • The Mesoproterozoic Iqqittuq Formation of the Borden basin (formerly part of the Society
518 Cliffs Formation) contains bedded gypsum deposits (massive and laminated with beds that
519 reach a thickness of 2.5 meters) and shale with halite casts (Kah et al., 2001). These
520 deposits are bracketed between Re-Os dates of 1048 ± 12 Ma for an underlying shale and
521 1046 ± 16 Ma for an overlying shale (Gibson et al., 2018).
- 522 • The Tonian Ten Stone Formation of the Mackenzie Mountains Supergroup (formerly known
523 as the Gypsum Formation) contains a ~500 meter thick successions dominated by gypsum
524 with minor anhydrite interpreted to have been deposited in a deep-water (below wave base)
525 restricted marine basin (Turner and Bekker, 2016). These thick bedded sulfate deposits are
526 older than cross-cutting 777.7 ± 2.5 Ma sills of the Gunbarrel large igneous province (U-Pb
527 date from Jefferson and Parrish, 1989) and younger than ca. 1005 Ma detrital zircons
528 (Turner and Bekker, 2016). The overlying Ram Head Formation has been correlated with
529 the Bitter Springs Stage which is constrained between 811.5 ± 0.3 Ma and 788.7 ± 0.2 Ma
530 (Macdonald et al., 2010; Swanson-Hysell et al., 2015) suggesting that the evaporites are ca.
531 820 Ma (Turner and Bekker, 2016). These deposits are hypothesized to be correlative with

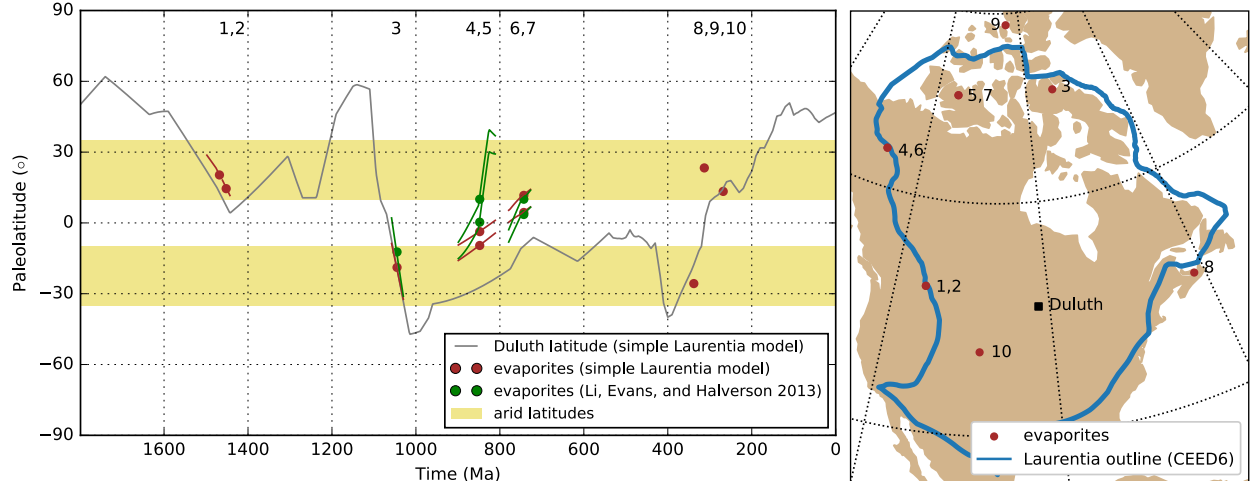


Figure 6. Left panel: The paleolatitude of evaporite deposits following the amalgamation of Laurentia as reconstructed by the simple Laurentia model shown in Fig. 5 combined with the Phanerozoic model of Torsvik and Cocks (2017) and as reconstructed by the model of Li et al. (2013) for the Neoproterozoic. Proterozoic evaporite deposits in this panel are discussed in the text while Phanerozoic ones are taken from the compilation of Evans (2006). The evaporite lines extend from the maximum to minimum age constraints while the points are at the preferred depositional age. Right panel: The present-day location of evaporites reconstructed to the left. 1: Altyn Formation (Belt Supergroup), 2: Wallace/Helena Formations (Belt Supergroup), 3: Iqqittuq Formation (Bylot Supergroup), 4: Ten Stone Formation (Mackenzie Mountains Supergroup), 5: Minto Inlet Formation (Shaler Supergroup), 6: Redstone River Formation (Mackenzie Mountains Supergroup), 7: Kilian Formation (Shaler Supergroup), 8: Carboniferous Canadian Maritime, 9: Carboniferous Sverdrup, 10: Permian Midcontinental USA.

532 sulfate evaporites within the Minto Inlet Formation of the Shaler Supergroup (Jones et al.,
 533 2010; Turner and Bekker, 2016).

- 534 • The Tonian Kilian Formation of the Shaler Supergroup contains nodules of gypsum and
 535 anhydrite interpreted to have been deposited in intertidal to supratidal evaporitic mudflat
 536 environment (Prince, 2014). The Kilian Formation is interpreted to post-date the Bitter
 537 Springs Stage and be correlative with the Redstone River Formation of the Coates Lake
 538 Group in the McKenzie Mountains that contains bedded gypsum as well as gypsum-bearing
 539 siltstone(Jefferson and Parrish, 1989; Jones et al., 2010). The Redstone River Formation is
 540 younger than the 777.7 ± 2.5 Ma volcanics and older than a 732.2 ± 4.7 Ma Re-Os isochron
 541 from the overlying Coppercap Formation.

542 In Figure 6, the paleolatitude of these evaporite deposits are reconstructed using the

543 **4.7 Comparing paleogeographic models to the paleomagnetic compilation**

544 Developing comprehensive global continuous paleogeographic models is a major challenge given
545 the need to integrate and satisfy diverse geological and paleomagnetic data types. Continually
546 improving constraints related to tectonic setting from improved geologic and geochronologic data
547 need to be carefully integrated with the database of paleomagnetic poles. Paleomagnetic pole
548 compilations themselves are evolving with better data and improved geochronology. Efforts such
549 as this volume are therefore essential to present the state-of-the-art in terms of existing
550 constraints that can be used to evaluate current models and set the stage for future progress in
551 Precambrian paleogeography.

552 There is an overall lack of models in the literature for the Proterozoic with published
553 continuous rotation parameters that can be compared to the compilation of paleomagnetic poles
554 presented herein. The approach in the community for many years has been to publish models as
555 snapshots at given time intervals presented in figures without publishing continuous rotation
556 parameters, although some studies have published the Euler rotations associated with specified
557 times. With the further adoption of software tools such as GPlates, there has been significant
558 progress in the publication of continuous paleogeographic models constrained by paleomagnetic
559 poles through the Phanerozoic (540 Ma to present; e.g. Torsvik et al., 2012).

560 An exception to the paucity of published continuous paleogeographic models for the
561 Precambrian is the Neoproterozoic model of Merdith et al. (2017) which is shown in comparison
562 to the constraints for Laurentia in Figure 5. The extent to which the implied position of
563 Laurentia in Merdith et al. (2017) is consistent with the compiled paleomagnetic constraints can
564 be visualized in Figure 5. As noted above, the development of such models is challenging and the
565 researchers need to balance varying constraints. The focus here will be on the extent to which
566 this model satisfies the available paleomagnetic poles for Laurentia. The model does not honor
567 the Grenville loop (e.g. Laurentia going to moderately high southerly latitudes ca. 1000 Ma),
568 which is a striking departure from the paleomagnetic record and standard paleogeographic
569 models. Additionally, the implemented plate motion strays from the younger poles of the
570 Keweenawan Track and does not honor the Franklin LIP pole Denyszyn et al. (2009b) despite its

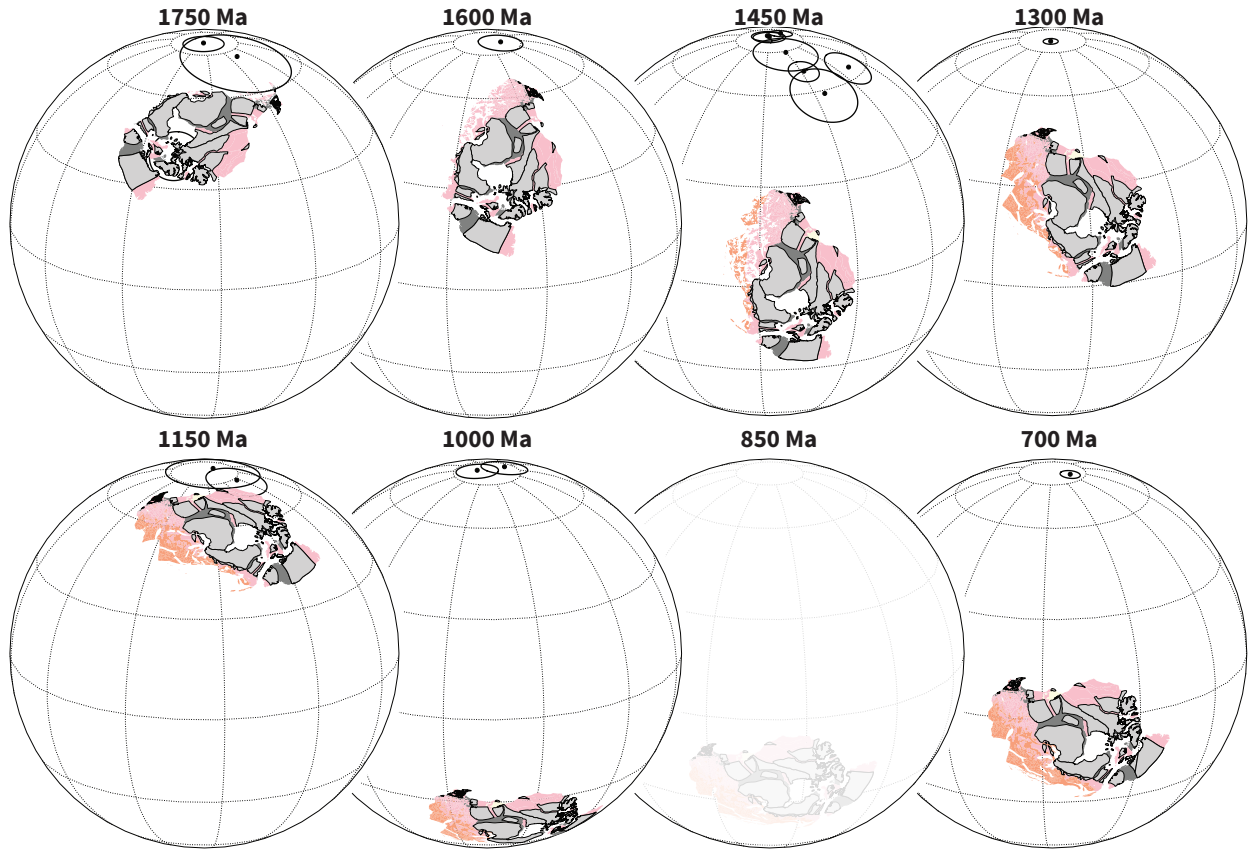


Figure 7. Paleogeographic reconstructions of Laurentia at time intervals through the Proterozoic that are well-constrained by paleomagnetic data. These reconstructions use the simple Laurentia pole interpolation model that is shown in Figure 5 and use this model to reconstruct the tectonic elements of Whitmeyer and Karlstrom (2007) shown in Figure 1. Modern coastlines are maintained in these polygons so that the rotated orientations can be interpreted by the reader in comparison to Figure 1. Paleomagnetic poles within 25 million years of each reconstruction time are plotted. All reconstructions have poles within such a time frame that provide constraints with the exception of the 850 Ma reconstruction which is shown faintly given this relative uncertainty in Laurentia's position.

571 ‘A’ Nordic rating. The Franklin pole is taken to be a key constraint at the Tonian/Cryogenian
572 boundary that provides evidence both for the supercontinent Rodinia being equatorial and for ice
573 sheets associated with the Sturtian glaciation having extended to equatorial latitudes (Macdonald
574 et al., 2010).

575 There are more published models that show snapshots and publish rotation parameters
576 associated with given time intervals such as the Rodinia model of Li et al. (2008) and the
577 Mesoproterozoic model of Pisarevsky et al. (2014), without providing parameters for a continuous
578 model. The position for Laurentia implied by the Euler poles given for the model snapshots of
579 these studies are shown in Figure 5 and can be compared to the compiled record. The figure also
580 shows the continuous implied position of Laurentia from the late Mesoproterozoic into the early
581 Paleozoic from the model of (Li et al., 2013; while the model parameters were not published with
582 that study they have now been made available by the authors).

583 4.8 Evaluating Laurentia’s Proterozoic paleogeographic neighbors

584 Many different paleogeographic connections between Laurentia and other Proterozoic cratons that
585 have been proposed and utilized in paleogeographic models. This section does not seek to be
586 comprehensive in this regard, but rather I seek to highlight and contextualize some of the more
587 prominent and/or well-supported models. *Note that this section is currently under development*
588 *and is incomplete*

589 4.8.1 Amazonia

590 In the central and southern Appalachians there are inliers of rocks that were metamorphosed
591 during the Ottawan phase of the Grenvillian orogeny (McLelland et al., 2013). On the basis of
592 whole-rock Pb-isotope data, Loewy et al. (2003) and Fisher et al. (2010) proposed that these
593 inliers are fragments of Amazonia lithosphere that were transferred to Laurentia during the
594 orogeny and left behind when the Iapetus Ocean formed. In particular, Fisher et al. (2010)
595 suggest the Sunsás orogen of Amazonia as the best match for southern and central Appalachian
596 inliers. This positioning leads to a paleogeographic model wherein Amazonia is a major portion of

597 the conjugate continental lithosphere that collided with Laurentia during Rodinia assembly
598 (Evans et al., 2013; Cawood and Pisarevsky, 2017). While the lack of ca. 1100 and ca. 1000 Ma
599 poles from Amazonia precludes a robust paleomagnetic test, this scenario is consistent with the
600 available late Mesoproterozoic poles from Amazonia (ca. 1200 Nova Floresta pole and ca. 1150
601 Fortuna Formation pole; D’Agrella-Filho et al., this volume) as shown in Evans et al. (2013). In
602 this paleogeographic scenario, the basement inliers of the Appalachian Orogen in the Blue Ridge
603 region are interpreted to be the leading edge of Amazonia with initial collision ca. 1080 initiating
604 the Ottawan phase of the Grenvillian orogeny (Fig. 2). Subsequent separation of Amazonia would
605 have lead to the formation of the Iapetus Ocean as Rodinia rifted apart. Departure of Amazonia
606 potentially occurred as early as ca. 700 Ma in the Paleo-Iapetus Ocean model of Robert et al.
607 (2020).

608 4.8.2 Baltica

609 Based on correlation of Archean provinces and Paleoproterozoic orogenic belts, Gower et al.
610 (1990) reconstructed Baltica to Laurentia in a position known as the NENA (northern Europe and
611 North America) configuration. This connection proposes a tight fit between modern-day northern
612 Norway and Russia’s Kola Peninsula with eastern Greenland (Gower et al., 1990, Salminen et al.,
613 this volume). In this position, Baltica and Laurentia are hypothesized to share a long-lived
614 accretionary margin (Karlstrom et al., 2001). This reconstruction is brings paleomagnetic poles
615 compatible with existing paleomagnetic constraints from ca. 1750 to 1270 Ma Evans and
616 Pisarevsky (2008) and these conjoined cratons feature as a major component of the hypothesized
617 Nuna supercontinent (Evans and Mitchell, 2011; Zhang et al., 2012; .

618 4.8.3 North China

619 The latest Mesoproterozoic to earliest Neoproterozoic pole path of the North China craton
620 includes a swath of paleomagnetic poles with a similar arc length to the Keweenawan Track to
621 Grenville Loop of Laurentia’s APWP (Zhao et al., 2019; Zhang et al., this volume). While the
622 chronostratigraphic age constraints on these North China poles are much looser than those from

623 Laurentia, Zhao et al. (2019) propose that the North China poles can be aligned with the
624 Keweenawan Track to reconstruct North China as being conjoined to the northwest margin of
625 Laurentia from prior to ca. 1110 Ma into the early Neoproterozoic. North China would have been
626 at polar latitudes ca. 1110 Ma and moved rapidly with Laurentia as it transited towards the
627 equator. Zhao et al. (2019) also argued that similarity in the detrital zircon age spectra between
628 early Neoproterozoic sediments in NW Laurentia and North China basins supports this
629 reconstruction. In particular, sediment transport from Laurentia could provide a source for ca.
630 1.18 Ga zircons (from the Shawinigan orogen) and ca. 1.08 Ga zircons (from the Grenville
631 orogen). In the Laurentia basins, ca. 1.6 Ga zircons without a clear Laurentia source could be
632 sourced from North China craton granites (e.g. Wang et al., 2020). If North China was in this
633 position, the timing of its arrival adjacent to Laurentia is unclear. The ca. 1220 Ma dikes pole of
634 the North China craton is not coincident with the ca. 1237 Ma Sudbury dikes pole in this
635 reconstructed position leading Zhao et al. (2019) and Zhang et al. (this volume) to suggest that
636 North China arrived on the Laurentian margin between ca. 1220 and 1110 Ma although they note
637 a lack of evidence for known North China orogenesis at this time. In terms of departing from this
638 position, one possibility is that its departure is associated with early Neoproterozoic extension in
639 northwest Laurentia.

640 4.9 The record implies plate tectonics throughout the Proterozoic

641 There is strong evidence both in Laurentia's geological and paleomagnetic record for differential
642 plate tectonic motion between 2.2 and 1.8 Ga. The continued history of accretionary orogenesis
643 and the evaluation of Laurentia's pole path in comparison to other continents from 1.8 Ga onward
644 supports the continual operation of plate tectonics throughout the rest of the Proterozoic and
645 Phanerozoic as well. While this evidence fits with the majority of interpretations of the timing of
646 initiation of modern-style plate tectonics (see summary in Korenaga, 2013), there continue to be
647 arguments proposing that a stagnant lid persisted through the Mesoproterozoic Era (1.6 to 1.0
648 Ga) and into the Neoproterozoic with plate tectonics not initiating until ca. 0.8 Ga (Hamilton,
649 2011; Stern and Miller, 2018). These arguments rest largely on the relative lack of Proterozoic
650 low-temperature high-pressure metamorphic rocks such as blueschists that form in subduction

651 zones (Stern et al., 2013). An alternative interpretation for this lack of blueschists in the
652 Proterozoic is that such a shift in metamorphic regime is the predicted result of secular evolution
653 of mantle chemistry rather than a harbinger of the onset of plate tectonics (Palin and White,
654 2015). While this line of evidence is intriguing, to argue that there was not differential plate
655 tectonic motion in the Paleoproterozoic and Mesoproterozoic is to ignore a vast breadth and depth
656 of geological and paleomagnetic data. From a paleomagnetic perspective, there is strong support
657 for independent and differential motion of the Slave and Superior provinces as is illustrated in
658 Figure 4. From a geological perspective, the Trans-Hudson orogenic cycle, the Grenville orogenic
659 cycle, and the Appalachian orogenic cycle are all well-explained with a mobilistic interpretation
660 that includes phases of accretionary followed by collisional orogenesis (Fig. 2). One could counter
661 that this perspective results from a plate-tectonic-centric viewpoint that lacks creativity to see
662 the record as resulting from other processes than modern-style plate tectonics. However, in
663 addition to the broad geological record showing an amalgamation of terranes as would be
664 expected to arise through plate tectonics, there are also an obducted ophiolite as well as eclogites
665 preserved in the Trans-Hudson orogen (Weller and St-Onge, 2017). These eclogites preserve
666 evidence for high-pressure/low-temperature metamorphic conditions ca. 1.8 Ga. Similar to the
667 Himalayan orogen, these rocks are interpreted to be the result of deep continental subduction and
668 exhumation associated with convergent plate tectonics (Weller and St-Onge, 2017). Outside of
669 Laurentia, there are examples of eclogites with geochemical affinity to oceanic crust such as that
670 documented in the ca. 1.9 Ga Ubendian Belt of the Congo craton (Boniface et al., 2012).

671 Another perspective on Proterozoic tectonics, is that the record is one of intermittent
672 subduction (Silver and Behn, 2008; O'Neill et al., 2013). In such a model, there are extended
673 intervals with a stagnant lid alternating with intervals of differential plate motion. In particular,
674 it has been argued that the Mesoproterozoic Era (1.6 to 1.0 Ga) is an interval when Earth was in
675 a stagnant regime (Silver and Behn, 2008; O'Neill et al., 2013). The long-lived accretionary
676 history of Laurentia following the amalgamation of the Archean provinces is difficult to reconcile
677 with such an interpretation (Figs. 1 and 2).

678 An additional constraint supporting ongoing plate tectonics throughout the Proterozoic comes
679 from the paleomagnetic record — in particular the paleomagnetic poles supported with baked

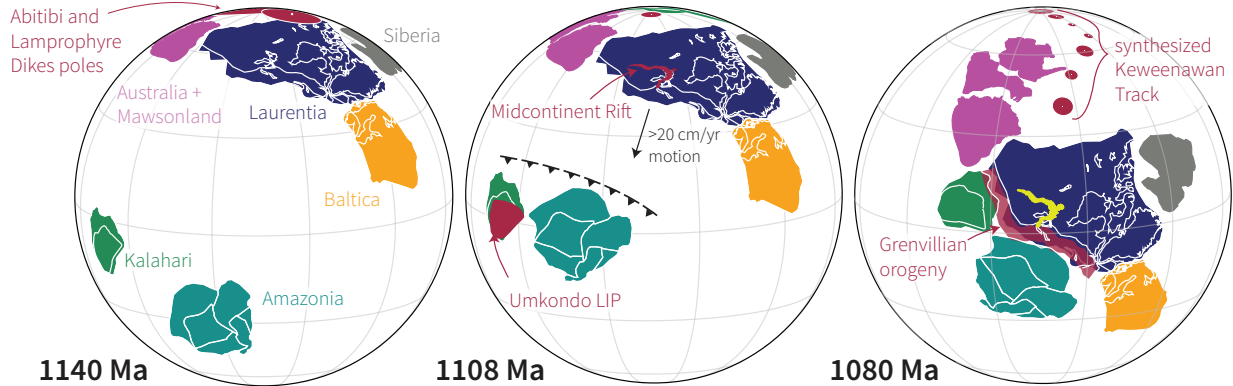


Figure 8. Paleogeographic reconstructions of Laurentia and other select Proterozoic continents leading up to Rodinia assembly in the late Mesoproterozoic modified from Swanson-Hysell et al. (2019). The record of paleomagnetic poles implies rapid motion which is consistent with the timing of collisional orogenesis associated with the Grenvillian orogeny.

680 contact tests (Fig. ??). In a stagnant lid regime, there would not be sufficient heat flow across
 681 the core-mantle boundary to sustain a geodynamo (Nimmo and Stevenson, 2000; Buffett, 2000).
 682 Baked contact tests indicate that, at the time of dike emplacement, there was an appreciable field
 683 such that both the cooling magma and the heated country rock in the vicinity of a dike were able
 684 to acquire a primary coherent magnetization direction. Additionally, since paleomagnetic poles
 685 are developed from many individual cooling units across a region, the similarity of the directions
 686 across an igneous province indicates that the magnetizations were dominantly acquired from the
 687 geomagnetic field rather than being influenced by local variable crustal magnetizations.
 688 Therefore, the record supports the persistence of a geomagnetic field through the Paleoproterozoic
 689 and Mesoproterozoic (Table 2) which implies active plate tectonics that enabled sufficient
 690 core-mantle boundary heat flow to power the geodynamo. This interpretation of a significant
 691 persistent geomagnetic field through much of the Proterozoic (with the potential exception of the
 692 Ediacaran; Bono et al., 2019) is further bolstered by estimates of paleointensity obtained from
 693 mafic dikes from Laurentia (e.g. Macouin et al., 2006) and elsewhere.
 694 The record of these poles also show that there was progressive motion of Laurentia through the
 695 Proterozoic (Figs. 5 and 7). Using data from Laurentia alone, however, it is difficult to ascertain
 696 whether this motion is due to plate tectonic motion or rotation of the entire solid Earth through
 697 true polar wander. True polar wander can lead to changing position relative to the spin axis even
 698 with a stagnant lid. One interval when the Laurentian paleomagnetic record demands that some

699 of the motion is through differential plate tectonics is in the latest Mesoproterozoic. At that time,
700 the pole path is very well-resolved with many high-quality paleomagnetic poles between 1110 and
701 1070 Ma (Table 2; 3). The progression of the poles requires rotation about an Euler pole that is
702 distinct from a great circle path which would result if the motion were solely due to true polar
703 wander (Swanson-Hysell et al., 2019). These poles constrain rapid motion of Laurentia leading up
704 to collisional orogenesis associated with the Grenvillian orogeny, as illustrated in Figure 8. These
705 data provide strong evidence for differential plate motion at the time and are inconsistent with a
706 stagnant lid. Rather, the orogenic cycle of the Mesoproterozoic bears similarity with that of the
707 Paleozoic and reveals Laurentia to have been a central player in the building of amalgamated
708 continents associated with Rodinia and Pangea.

709 4.10 Conclusion

710 The paleogeographic record of Laurentia is rich in constraints through the Precambrian both in
711 terms of the geological and geochronological constraints on tectonism and the record of
712 paleomagnetic poles. Data from the Slave and Superior provinces of Laurentia provide what is
713 arguably the strongest evidence of differential plate tectonics in the Rhyacian and Orosirian
714 Periods of the Paleoproterozoic Era (2.3 to 1.8 Ga) leading up to the collision of these terranes
715 during the Trans-Hudson orogeny. The collisions of these and other Archean provinces led to the
716 formation of the core of Laurentia. Subsequent crustal growth occurred through multiple intervals
717 of accretionary orogenesis through the late Paleoproterozoic and Mesoproterozoic until the
718 continent-continent collision of the Grenvillian orogeny that was ongoing at the
719 Mesoproterozoic-Neoproterozoic boundary (1.0 Ga). The lead-up to this orogeny was associated
720 with rapid plate motion of Laurentia from high latitudes towards the equator recorded by the
721 Logan Loop and Keweenawan Track of paleomagnetic poles. Following, a return to high latitudes
722 as constrained by paleomagnetic poles of the Grenville Loop, Laurentia straddled the equator at
723 the time of Cryogenian Snowball Earth glaciation as part of the Rodinia supercontinent. Rifting
724 and passive margin development then isolated Laurentia in the early Paleozoic Era. Subsequent
725 accretionary and collisional orogenesis occurred associated with the Appalachian orogenic cycle
726 with Laurentia first colliding with Avalonia-Baltica to become Laurussia and Laurussia then

727 uniting with Gondwana to form Pangea. While the details of the conjugate continents are better
728 reconstructed for this last Wilson cycle, the broad features of the Trans-Hudson, Grenvillian and
729 Appalachian orogenic cycles bear similarities. In each case, accretionary collision of arc terranes
730 was followed by continent-continent collision. The major difference is that the collisions of the
731 Grenvillian and Appalachian orogenic cycles resulted in relatively minor crustal growth compared
732 to the Trans-Hudson. Break-up following the Grenvillian and Appalachian orogenic cycles
733 occurred along the same margin as collision while the major orogens of the Trans-Hudson orogenic
734 cycle have remained sutured. As a result, Laurentia has been a formidable continent for the past
735 1.8 billion years. As can be seen in the Chapters on Archean paleogeography (Salminen et al.,
736 this volume), Nuna (Elming et al., this volume) and Rodinia (Evans et al., this volume), the
737 constraints from Laurentia are at the center of paleogeographic models through the Precambrian
738 and will continue to be as the next generation of paleogeographic models are developed.

739 Acknowledgements

740 Many participants in the Nordic Paleomagnetism Workshop have contributed to the compilation
741 and evaluation of the pole list utilized herein. Particular acknowledgement goes to David Evans
742 for maintaining and distributing the compiled pole lists as well as additional efforts of Lauri
743 Pesonen in maintaining the Paleomagia database (Veikkolainen et al., 2014). GPlates, and in
744 particular the pyGPlates API, was utilized in this work (Müller et al., 2018). Figures were made
745 using Matplotlib (Hunter, 2007) in conjunction with cartopy (Met Office, 2010 - 2015) and
746 pmagpy (Tauxe et al., 2016) within an interactive Python environment (Pérez and Granger,
747 2007). The manuscript benefited from reviews from Athena Eyster, David Evans, and Lauri
748 Pesonen as well as discussions with Francis Macdonald. This work was supported by NSF
749 CAREER Grant EAR-1847277 awarded to N.L.S.-H. The chapter text as well as code, data, and
750 reconstructions used in this paper are openly available and licensed for any form of reuse (CC BY
751 4.0) with attribution in this repository:
752 https://github.com/Swanson-Hysell-Group/Laurentia_Paleogeography.

753 **References**

- 754 Abrahamsen, N. and Van Der Voo, R., 1987, Palaeomagnetism of middle Proterozoic (c. 1.25 Ga) dykes from central
755 North Greenland: *Geophysical Journal International*, v. 91, p. 597–611, doi:10.1111/j.1365-246x.1987.tb01660.x.
- 756 Abrajevitch, A. and Van der Voo, R., 2010, Incompatible Ediacaran paleomagnetic directions suggest an equatorial
757 geomagnetic dipole hypothesis: *Earth and Planetary Science Letters*, v. 293, p. 164–170.
- 758 Bates, M. P. and Halls, H. C., 1991, Broad-scale Proterozoic deformation of the central Superior Province revealed
759 by paleomagnetism of the 2.45 Ga Matachewan dyke swarm: *Canadian Journal of Earth Sciences*, v. 28, p.
760 1780–1796, doi:10.1139/e91-159.
- 761 Berman, R., Davis, A., and Pehrsson, S., 2007, Collisional Snowbird tectonic zone resurrected: Growth of Laurentia
762 during the 1.9 Ga accretionary phase of the Hudsonian orogeny: *Geology*, v. 35, p. 911–914,
763 doi:10.1130/G23771A.1.
- 764 Bickford, M., Van Schmus, W., Karlstrom, K., Mueller, P., and Kamenov, G., 2015,
765 Mesoproterozoic-trans-Laurentian magmatism: A synthesis of continent-wide age distributions, new SIMS U–Pb
766 ages, zircon saturation temperatures, and Hf and Nd isotopic compositions: *Precambrian Research*, v. 265, p.
767 286–312, doi:10.1016/j.precamres.2014.11.024.
- 768 Bond, G., Nickleson, P., and Kominz, M., 1984, Breakup of a supercontinent between 625 and 555 Ma: new
769 evidence and implications for continental histories: *Earth and Planetary Science Letters*, v. 70, p. 325–345,
770 doi:10.1016/0012-821X(84)90017-7.
- 771 Boniface, N., Schenk, V., and Appel, P., 2012, Paleoproterozoic eclogites of MORB-type chemistry and three
772 Proterozoic orogenic cycles in the Ubendian Belt (Tanzania): Evidence from monazite and zircon geochronology,
773 and geochemistry: *Precambrian Research*, v. 192–195, p. 16–33, doi:10.1016/j.precamres.2011.10.007.
- 774 Bono, R. K. and Tarduno, J. A., 2015, A stable Ediacaran Earth recorded by single silicate crystals of the ca. 565
775 Ma Sept-Îles intrusion: *Geology*, v. 43, p. 131–134, doi:10.1130/G36247.1.
- 776 Bono, R. K., Tarduno, J. A., Nimmo, F., and Cottrell, R. D., 2019, Young inner core inferred from Ediacaran
777 ultra-low geomagnetic field intensity: *Nature Geoscience*, v. 12, p. 143–147, doi:10.1038/s41561-018-0288-0.
- 778 Books, K., 1972, Paleomagnetism of some Lake Superior Keweenawan rocks: U.S. Geological Survey Professional
779 Paper, v. P 0760, p. 42.
- 780 Borradaile, G. and Middleton, R., 2006, Proterozoic paleomagnetism in the Nipigon Embayment of northern
781 Ontario: Pillar Lake Lava, Wawieg Troctolite and Gunflint Formation tuffs: *Precambrian Research*, v. 144, p.
782 69–91, doi:10.1016/j.precamres.2005.10.007.

- 783 Brown, L. L. and McEnroe, S. A., 2012, Paleomagnetism and magnetic mineralogy of Grenville metamorphic and
784 igneous rocks, Adirondack Highlands, USA: Precambrian Research, v. 212–213, p. 57–74,
785 doi:10.1016/j.precamres.2012.04.012.
- 786 Buchan, K., Mertanen, S., Park, R., Pesonen, L., Elming, S. A., Abrahamsen, N., and Bylund, G., 2000, Comparing
787 the drift of Laurentia and Baltica in the Proterozoic: the importance of key paleomagnetic poles:
788 Tectonophysics, v. 319, p. 167–198.
- 789 Buchan, K. L., LeCheminant, A. N., and van Breemen, O., 2009, Paleomagnetism and U–Pb geochronology of the
790 Lac de Gras diabase dyke swarm, Slave Province, Canada: implications for relative drift of Slave and Superior
791 provinces in the Paleoproterozoic: Canadian Journal of Earth Sciences, v. 46, p. 361–379, doi:10.1139/e09-026.
- 792 Buchan, K. L., LeCheminant, A. N., and van Breemen, O., 2012, Malley diabase dykes of the Slave craton,
793 Canadian Shield: U–Pb age, paleomagnetism, and implications for continental reconstructions in the early
794 Paleoproterozoic: Canadian Journal of Earth Sciences, v. 49, p. 435–454, doi:10.1139/e11-061.
- 795 Buchan, K. L., Mitchell, R. N., Bleeker, W., Hamilton, M. A., and LeCheminant, A. N., 2016, Paleomagnetism of
796 ca. 2.13–2.11 Ga Indin and ca. 1.885 Ga Ghost dyke swarms of the Slave craton: Implications for the Slave
797 craton APW path and relative drift of Slave, Superior and Siberian cratons in the Paleoproterozoic: Precambrian
798 Research, v. 275, p. 151–175, doi:10.1016/j.precamres.2016.01.012.
- 799 Buchan, K. L., Mortensen, J. K., and Card, K. D., 1993, Northeast-trending early Proterozoic dykes of southern
800 Superior Province: multiple episodes of emplacement recognized from integrated paleomagnetism and U–Pb
801 geochronology: Canadian Journal of Earth Sciences, v. 30, p. 1286–1296, doi:10.1139/e93-110.
- 802 Buffett, B. A., 2000, Earth's core and the geodynamo: Science, v. 288, p. 2007–2012.
- 803 Burls, N. J. and Fedorov, A. V., 2017, Wetter subtropics in a warmer world: Contrasting past and future
804 hydrological cycles: Proceedings of the National Academy of Sciences, v. 114, p. 12,888–12,893,
805 doi:10.1073/pnas.1703421114.
- 806 Burton, W. C. and Southworth, S., 2010, A model for Iapetan rifting of Laurentia based on Neoproterozoic dikes
807 and related rocks: From Rodinia to Pangea: The Lithotectonic Record of the Appalachian Region, p. 455–476,
808 doi:10.1130/2010.1206(20).
- 809 Cannon, W. F., 1992, The Midcontinent rift in the Lake Superior region with emphasis on its geodynamic
810 evolution: Tectonophysics, v. 213, p. 41–48, doi:10.1016/0040-1951(92)90250-A.
- 811 Cawood, P. A. and Pisarevsky, S. A., 2017, Laurentia-baltica-amazonia relations during rodinia assembly:
812 Precambrian Research, p. –, doi:<http://dx.doi.org/10.1016/j.precamres.2017.01.031>.

- 813 Chiarenzelli, J., Lupulescu, M., Thern, E., and Cousens, B., 2011, Tectonic implications of the discovery of a
814 Shawinigan ophiolite (Pyrites Complex) in the Adirondack Lowlands: *Geosphere*, v. 7, p. 333–356,
815 doi:10.1130/ges00608.1.
- 816 Condit, C. B., Mahan, K. H., Ault, A. K., and Flowers, R. M., 2015, Foreland-directed propagation of high-grade
817 tectonism in the deep roots of a Paleoproterozoic collisional orogen, SW Montana, USA: *Lithosphere*, p. L460.1,
818 doi:10.1130/l460.1.
- 819 Corrigan, D., Pehrsson, S., Wodicka, N., and de Kemp, E., 2009, The Palaeoproterozoic Trans-Hudson Orogen: a
820 prototype of modern accretionary processes: Geological Society, London, Special Publications, v. 327, p. 457–479,
821 doi:10.1144/sp327.19.
- 822 Dahl, P. S., Holm, D. K., Gardner, E. T., Hubacher, F. A., and Foland, K. A., 1999, New constraints on the timing
823 of Early Proterozoic tectonism in the Black Hills (South Dakota), with implications for docking of the Wyoming
824 province with Laurentia: *Geological Society of America Bulletin*, v. 111, p. 1335–1349,
825 doi:10.1130/0016-7606(1999)111<1335:ncotto>2.3.co;2.
- 826 Daniel, C. G., Pfeifer, L. S., Jones, J. V., and McFarlane, C. M., 2013, Detrital zircon evidence for non-Laurentian
827 provenance, Mesoproterozoic (ca. 1490–1450 Ma) deposition and orogenesis in a reconstructed orogenic belt,
828 northern New Mexico, USA: Defining the Picuris orogeny: *Geological Society of America Bulletin*, v. 125, p.
829 1423–1441, doi:10.1130/b30804.1.
- 830 Dehler, C., Gehrels, G., Porter, S., Heizler, M., Karlstrom, K., Cox, G., Crossey, L., and Timmons, M., 2017,
831 Synthesis of the 780–740 ma chuar, uinta mountain, and pahrump (chump) groups, western usa: Implications for
832 laurentia-wide cratonic marine basins: *Geological Society of America Bulletin*, v. 129, p. 607–624,
833 doi:10.1130/b31532.1.
- 834 Denyszyn, S. W., Davis, D. W., and Halls, H. C., 2009a, Paleomagnetism and U–Pb geochronology of the Clarence
835 Head dykes, Arctic Canada: orthogonal emplacement of mafic dykes in a large igneous province: *Canadian*
836 *Journal of Earth Sciences*, v. 46, p. 155–167, doi:10.1139/E09-011.
- 837 Denyszyn, S. W., Halls, H. C., Davis, D. W., and Evans, D. A. D., 2009b, Paleomagnetism and U–Pb geochronology
838 of Franklin dykes in High Arctic Canada and Greenland: a revised age and paleomagnetic pole constraining block
839 rotations in the Nares Strait region: *Canadian Journal of Earth Sciences*, v. 46, p. 689–705, doi:10.1139/E09-042.
- 840 Dickerson, P. W. and Keller, M., 1998, The Argentine Precordillera: its odyssey from the Laurentian Ouachita
841 margin towards the Sierras Pampeanas of Gondwana: Geological Society, London, Special Publications, v. 142,
842 p. 85–105, doi:10.1144/gsl.sp.1998.142.01.05.
- 843 Donadini, F., Pesonen, L. J., Korhonen, K., Deutsch, A., and Harlan, S. S., 2011, Paleomagnetism and
844 paleointensity of the 1.1 Ga old diabase sheets from central Arizona: *Geophysica*, v. 47, p. 3–30.

- 845 Elming, S. Å., D'Aarella-Filho, M. S., Page, L. M., Tohver, E., Trindade, R. I. F., Pacca, I. I. G., Geraldes, M. C.,
846 and Teixeira, W., 2009, A palaeomagnetic and 40Ar/39Ar study of late precambrian sills in the SW part of the
847 Amazonian craton: Amazonia in the Rodinia reconstruction: Geophysical Journal International, v. 178, p.
848 106–122.
- 849 Elston, D. P., Enkin, R. J., Baker, J., and Kisilevsky, D. K., 2002, Tightening the Belt: Paleomagnetic-stratigraphic
850 constraints on deposition, correlation, and deformation of the Middle Proterozoic (ca. 1.4 Ga) Belt-Purcell
851 Supergroup, United States and Canada: GSA Bulletin, v. 114, p. 619–638,
852 doi:10.1130/0016-7606(2002)114<0619:TTBPSC>2.0.CO;2.
- 853 Emslie, R. F., Irving, E., and Park, J. K., 1976, Further paleomagnetic results from the Michikamau Intrusion,
854 Labrador: Canadian Journal of Earth Sciences, v. 13, p. 1052–1057, doi:10.1139/e76-108.
- 855 Ernst, R. and Buchan, K., 1993, Paleomagnetism of the Abitibi dike swarm, southern Superior Province, and
856 implications for the Logan Loop: Canadian Journal of Earth Science, v. 30, p. 1886–1897, doi:10.1139/e93-167.
- 857 Eugster, H., 1980, Chapter 15 lake magadi, kenya, and its precursors: In Developments in Sedimentology, Elsevier,
858 p. 195–232, doi:10.1016/s0070-4571(08)70239-5, URL
859 <https://doi.org/10.1016%2Fs0070-4571%2808%2970239-5>.
- 860 Evans, D., 2006, Proterozoic low orbital obliquity and axial-dipolar geomagnetic field from evaporite
861 palaeolatitudes: Nature, v. 444, p. 51–55.
- 862 Evans, D. and Halls, H., 2010, Restoring Proterozoic deformation within the Superior craton: Precambrian
863 Research, v. 183, p. 474 – 489, doi:10.1016/j.precamres.2010.02.007.
- 864 Evans, D. A. D. and Mitchell, R. N., 2011, Assembly and breakup of the core of Paleoproterozoic–Mesoproterozoic
865 supercontinent Nuna: Geology, v. 39, p. 443–446.
- 866 Evans, D. A. D. and Pisarevsky, S. A., 2008, Plate tectonics on early Earth? weighing the paleomagnetic evidence:
867 Geological Society of America Special Papers, v. 440, p. 249–263.
- 868 Evans, K. A., McCuaig, T. C., Leach, D., Angerer, T., and Hagemann, S. G., 2013, Banded iron formation to iron
869 ore: A record of the evolution of earth environments?: Geology, v. 41, p. 99–102.
- 870 Evans, K. V., Aleinikoff, J. N., Obradovich, J. D., and Fanning, C. M., 2000, SHRIMP U-Pb geochronology of
871 volcanic rocks, Belt Supergroup, western Montana: evidence for rapid deposition of sedimentary strata:
872 Canadian Journal of Earth Sciences, v. 37, p. 1287–1300, doi:10.1139/e00-036.
- 873 Evans, M. E. and Bingham, D. K., 1973, Paleomagnetism of the Precambrian Martin Formation, Saskatchewan:
874 Canadian Journal of Earth Sciences, v. 10, p. 1485–1493, doi:10.1139/e73-141.

- 875 Evans, M. E. and Heller, F., 2003, Environmental Magnetism: Principles and Applications of Enviromagnetics:
876 Academic Press.
- 877 Evans, M. E. and Hoye, G. S., 1981, Paleomagnetic results from the lower proterozoic rocks of Great Slave Lake and
878 Bathurst Inlet areas, Northwest Territories: *In* Proterozoic Basins of Canada; Geological Survey of Canada,
879 Paper 81-10, Natural Resources Canada/ESS/Scientific and Technical Publishing Services, doi:10.4095/109374.
- 880 Eyster, A., Weiss, B. P., Karlstrom, K., and Macdonald, F. A., 2019, Paleomagnetism of the Chuar Group and
881 evaluation of the late Tonian Laurentian apparent polar wander path with implications for the makeup and
882 breakup of Rodinia: *GSA Bulletin*, doi:10.1130/b32012.1.
- 883 Fahrig, W. and Bridgwater, D., 1976, Late Archean-early Proterozoic paleomagnetic pole positions from west
884 Greenland: *In* Windley, B., ed., Early History of the Earth, Wiley, p. 427–442.
- 885 Fahrig, W. F. and Jones, D. L., 1976, The paleomagnetism of the Helikian Mistastin pluton, Labrador, Canada:
886 Canadian Journal of Earth Sciences, v. 13, p. 832–837, doi:10.1139/e76-086.
- 887 Fairchild, L. M., Swanson-Hysell, N. L., Ramezani, J., Sprain, C. J., and Bowring, S. A., 2017, The end of
888 Midcontinent Rift magmatism and the paleogeography of Laurentia: *Lithosphere*, v. 9, p. 117–133,
889 doi:10.1130/L580.1.
- 890 Fisher, C. M., Loewy, S. L., Miller, C. F., Berquist, P., Van Schmus, W. R., Hatcher, R. D., Wooden, J. L., and
891 Fullagar, P. D., 2010, Whole-rock pb and sm-nd isotopic constraints on the growth of southeastern laurentia
892 during grenvillian orogenesis: *Geological Society of America Bulletin*, v. 122, p. 1646–1659, doi:10.1130/b30116.1.
- 893 Gala, M. G., Symons, D. T. A., and Palmer, H. C., 1995, Paleomagnetism of the Jan Lake Granite, Trans-Hudson
894 Orogen: *Saskatchewan Geological Survey Summary of Investigations*, v. 95-4.
- 895 Gibson, T. M., Shih, P. M., Cumming, V. M., Fischer, W. W., Crockford, P. W., Hodgskiss, M. S., Wörndl, S.,
896 Creaser, R. A., Rainbird, R. H., Skulski, T. M., and et al., 2018, Precise age of bangiomorpha pubescens dates
897 the origin of eukaryotic photosynthesis: *Geology*, doi:10.1130/g39829.1.
- 898 Gower, C. F., Ryan, A. B., and Rivers, T., 1990, Mid-Proterozoic Laurentia-Baltica: An overview of its geological
899 evolution and a summary of the contributions made by this volume: *In* Gower, C. F., Rivers, T., and Ryan,
900 A. B., eds., Mid-Proterozoic Laurentia-Baltica, Geological Association of Canada, Special Paper.
- 901 Grimes, S. W. and Copeland, P., 2004, Thermochronology of the grenville orogeny in west texas: *Precambrian*
902 *Research*, v. 131, p. 23–54, doi:10.1016/j.precamres.2003.12.004.
- 903 Halls, H., 1974, A paleomagnetic reversal in the Osler Volcanic Group, northern Lake Superior: *Canadian Journal*
904 *of Earth Science*, v. 11, p. 1200–1207, doi:10.1139/e74-113.

- 905 Halls, H. C., 2015, Paleomagnetic evidence for ~4000 km of crustal shortening across the 1 Ga Grenville orogen of
906 North America: *Geology*, v. 43, p. 1051–1054, doi:10.1130/G37188.1.
- 907 Halls, H. C., Davis, D. W., Stott, G. M., Ernst, R. E., and Hamilton, M. A., 2008, The Paleoproterozoic Marathon
908 Large Igneous Province: New evidence for a 2.1 Ga long-lived mantle plume event along the southern margin of
909 the North American Superior Province: *Precambrian Research*, v. 162, p. 327–353,
910 doi:10.1016/j.precamres.2007.10.009.
- 911 Halls, H. C., Hamilton, M. A., and Denyszyn, S. W., 2011, The Melville Bugt Dyke Swarm of Greenland: A
912 Connection to the 1.5-1.6 Ga Fennoscandian Rapakivi Granite Province?, Springer Berlin Heidelberg, p. 509–535:
913 doi:10.1007/978-3-642-12496-9{_}27.
- 914 Halls, H. C. and Hanes, J. A., 1999, Paleomagnetism, anisotropy of magnetic susceptibility, and argon–argon
915 geochronology of the Clearwater anorthosite, Saskatchewan, Canada: *Tectonophysics*, v. 312, p. 235–248,
916 doi:10.1016/s0040-1951(99)00166-3.
- 917 Halls, H. C., Lovette, A., Hamilton, M., and Söderlund, U., 2015, A paleomagnetic and u–pb geochronology study
918 of the western end of the grenville dyke swarm: Rapid changes in paleomagnetic field direction at ca.
919 585 ma related to polarity reversals?: *Precambrian Research*, v. 257, p. 137–166,
920 doi:<http://dx.doi.org/10.1016/j.precamres.2014.11.029>.
- 921 Halverson, G. P., Porter, S. M., and Gibson, T. M., 2018, Dating the late Proterozoic stratigraphic record:
922 Emerging Topics in Life Sciences, v. 2, p. 137–147, doi:10.1042/etls20170167.
- 923 Hamilton, W. B., 2011, Plate tectonics began in Neoproterozoic time, and plumes from deep mantle have never
924 operated: *Lithos*, v. 123, p. 1–20, doi:10.1016/j.lithos.2010.12.007.
- 925 Harlan, S., 1993, Paleomagnetism of Middle Proterozoic diabase sheets from central Arizona: *Canadian Journal of*
926 *Earth Science*, v. 30, p. 1415–1426.
- 927 Harlan, S., Geissman, J., and Snee, L., 1997, Paleomagnetic and $^{40}\text{Ar}/^{39}\text{Ar}$ geochronologic data from late
928 Proterozoic mafic dykes and sills, Montana and Wyoming: *USGS Professional Paper*, v. 1580, p. 16.
- 929 Harlan, S. S. and Geissman, J. W., 1998, Paleomagnetism of the middle Proterozoic Electra Lake Gabbro, Needle
930 Mountains, southwestern Colorado: *Journal of Geophysical Research: Solid Earth*, v. 103, p. 15,497–15,507,
931 doi:10.1029/98jb01350.
- 932 Harlan, S. S., Geissman, J. W., and Snee, L. W., 2008, Paleomagnetism of Proterozoic mafic dikes from the Tobacco
933 Root Mountains, southwest Montana: *Precambrian Research*, v. 163, p. 239–264.
- 934 Harlan, S. S., Snee, L. W., Geissman, J. W., and Brearley, A. J., 1994, Paleomagnetism of the middle proterozoic
935 laramie anorthosite complex and sherman granite, southern laramie range, wyoming and colorado: *Journal of*
936 *Geophysical Research: Solid Earth*, v. 99, p. 17,997–18,020, doi:10.1029/94jb00580.

- 937 Henry, S., Mauk, F., and Van der Voo, R., 1977, Paleomagnetism of the upper Keweenawan sediments: Nonesuch
938 Shale and Freda Sandstone: Canadian Journal of Earth Science, v. 14, p. 1128–1138, doi:10.1139/e77-103.
- 939 Hietanen, A., 1967, 86 : Scapolite in the belt series in the st. joe-clearwater region, idaho: GSA Special Papers,
940 doi:10.1130/spe86.
- 941 Hildebrand, R. S., Hoffman, P. F., and Bowring, S. A., 2009, The Calderian orogeny in Wopmay orogen (1.9 Ga),
942 northwestern Canadian Shield: Geological Society of America Bulletin, v. 122, p. 794–814, doi:10.1130/B26521.1.
- 943 Hnat, J. S., van der Pluijm, B. A., and Van der Voo, R., 2006, Primary curvature in the Mid-Continent Rift:
944 Paleomagnetism of the Portage Lake Volcanics (northern Michigan, USA): Tectonophysics, v. 425, p. 71–82,
945 doi:10.1016/j.tecto.2006.07.006.
- 946 Hoffman, P., 1991, Did the breakout of Laurentia turn Gondwana inside out?: Science, v. 252, p. 1409–1412.
- 947 Hoffman, P. F., 1988, United plates of America, the birth of a craton: Early Proterozoic assembly and growth of
948 Laurentia: Annual Review of Earth and Planetary Sciences, v. 16, p. 543–603,
949 doi:10.1146/annurev.ea.16.050188.002551.
- 950 Hoffman, P. F., 1989, Speculations on Laurentia's first gigayear (2.0 to 1.0 Ga): Geology, v. 17, p. 135–138,
951 doi:10.1130/0091-7613(1989)017<0135:SOLSGF>2.3.CO;2.
- 952 Hoffman, P. F., Halverson, G. P., Domack, E. W., Maloof, A. C., Swanson-Hysell, N. L., and Cox, G. M., 2012,
953 Cryogenian glaciations on the southern tropical paleomargin of Laurentia (NE Svalbard and East Greenland),
954 and a primary origin for the upper Russøya (Islay) carbon isotope excursion: Precambrian Research, v. 206–207,
955 p. 137–158, doi:10.1016/j.precamres.2012.02.018.
- 956 Holm, D. K., Van Schmus, W. R., MacNeill, L. C., Boerboom, T. J., Schweitzer, D., and Schneider, D., 2005, U-Pb
957 zircon geochronology of Paleoproterozoic plutons from the northern midcontinent, USA: Evidence for subduction
958 flip and continued convergence after geon 18 Penokean orogenesis: Geological Society of America Bulletin, v. 117,
959 p. 259, doi:10.1130/b25395.1.
- 960 Hrncir, J., Karlstrom, K., and Dahl, P., 2017, Wyoming on the run—Toward final Paleoproterozoic assembly of
961 Laurentia: COMMENT: Geology, v. 45, p. e411–e411, doi:10.1130/g38826c.1.
- 962 Hunter, J. D., 2007, Matplotlib: A 2D graphics environment: Computing in Science & Engineering, v. 9, p. 90–95,
963 doi:10.1109/MCSE.2007.55.
- 964 Hynes, A. and Rivers, T., 2010, Protracted continental collision — evidence from the Grenville Orogen: Canadian
965 Journal of Earth Sciences, v. 47, p. 591–620, doi:10.1139/e10-003.
- 966 Irving, E., 2004, Early Proterozoic geomagnetic field in western Laurentia: implications for paleolatitudes, local
967 rotations and stratigraphy: Precambrian Research, v. 129, p. 251–270, doi:10.1016/j.precamres.2003.10.002.

- 968 Irving, E. and McGlynn, J. C., 1979, Palaeomagnetism in the Coronation Geosyncline and arrangement of
969 continents in the middle Proterozoic: *Geophysical Journal International*, v. 58, p. 309–336,
970 doi:10.1111/j.1365-246X.1979.tb01027.x.
- 971 Irving, E. and Park, J. K., 1972, Hairpins and superintervals: *Canadian Journal of Earth Sciences*, v. 9, p.
972 1318–1324, doi:10.1139/e72-115.
- 973 Jefferson, C. W. and Parrish, R. R., 1989, Late proterozoic stratigraphy, u–pb zircon ages, and rift tectonics,
974 mackenzie mountains, northwestern canada: *Canadian Journal of Earth Sciences*, v. 26, p. 1784–1801.
- 975 Johnson, T. A., Vervoort, J. D., Ramsey, M. J., Southworth, S., and Mulcahy, S. R., 2020, Tectonic evolution of the
976 grenville orogen in the central appalachians: *Precambrian Research*, p. 105740,
977 doi:10.1016/j.precamres.2020.105740.
- 978 Jones, D. S., Maloof, A. C., Hurtgen, M. T., Rainbird, R. H., and Schrag, D. P., 2010, Regional and global
979 chemostratigraphic correlation of the early Neoproterozoic Shaler Supergroup, Victoria Island, Northwestern
980 Canada: *Precambrian Research*, v. 181, p. 43–63.
- 981 Jones, J. V., Daniel, C. G., and Doe, M. F., 2015, Tectonic and sedimentary linkages between the Belt-Purcell basin
982 and southwestern Laurentia during the Mesoproterozoic, ca. 1.60–1.40 Ga: *Lithosphere*, v. 7, p. 465–472,
983 doi:10.1130/l438.1.
- 984 Kah, L., Lyons, T., and Chesley, J., 2001, Geochemistry of a 1.2 ga carbonate-evaporite succession, northern baffin
985 and bylot islands: implications for mesoproterozoic marine evolution: *Precambrian Research*, v. 111, p. 203–234.
- 986 Karlstrom, K. E., Ahall, K.-I., Harlan, S. S., Williams, M. L., McLelland, J., and Geissman, J. W., 2001, Long-lived
987 (1.8-1.0 Ga) convergent orogen in southern Laurentia, its extensions to Australia and Baltica, and implications
988 for refining Rodinia: *Precambrian Research*, v. 111, p. 5–30, doi:10.1016/S0301-9268(01)00154-1.
- 989 Karlstrom, K. E. and Bowring, S. A., 1988, Early Proterozoic assembly of tectonostratigraphic terranes in
990 southwestern North America: *The Journal of Geology*, v. 96, p. 561–576, doi:10.1086/629252.
- 991 Kean, W., Williams, I., and Feeney, J., 1997, Magnetism of the Keweenawan age Chengwatana lava flows, northwest
992 Wisconsin: *Geophysical Research Letters*, v. 24, p. 1523–1526, doi:10.1029/97gl00993.
- 993 Kilian, T. M., Bleeker, W., Chamberlain, K., Evans, D. A. D., and Cousens, B., 2015, Palaeomagnetism,
994 geochronology and geochemistry of the Palaeoproterozoic Rabbit Creek and Powder River dyke swarms:
995 implications for Wyoming in supercraton Superia: *Geological Society, London, Special Publications*, v. 424, p.
996 15–45, doi:10.1144/sp424.7.
- 997 Kilian, T. M., Chamberlain, K. R., Evans, D. A., Bleeker, W., and Cousens, B. L., 2016, Wyoming on the
998 run—Toward final Paleoproterozoic assembly of Laurentia: *Geology*, v. 44, p. 863–866, doi:10.1130/g38042.1.

- 999 Korenaga, J., 2013, Initiation and evolution of plate tectonics on earth: Theories and observations: Annual Review
1000 of Earth and Planetary Sciences, v. 41, p. 117–151, doi:10.1146/annurev-earth-050212-124208.
- 1001 Kulakov, E. V., Smirnov, A. V., and Diehl, J. F., 2013, Paleomagnetism of ~1.09 Ga Lake Shore Traps (Keweenaw
1002 Peninsula, Michigan): new results and implications: Canadian Journal of Earth Sciences, v. 50, p. 1085–1096,
1003 doi:10.1139/cjes-2013-0003.
- 1004 Levy, M. and Christie-Blick, N., Nicholas, 1991, Tectonic subsidence of the early Paleozoic passive continental
1005 margin in eastern California and southern Nevada: Geological Society of America Bulletin, v. 103, p. 1590–1606,
1006 doi:10.1130/0016-7606(1991)103<1590:tsotep>2.3.co;2.
- 1007 Li, Z.-X., Evans, D. A. D., and Halverson, G., 2013, Neoproterozoic glaciations in a revised global palaeogeography
1008 from the breakup of Rodinia to the assembly of Gondwanaland: Sedimentary Geology, v. 294, p. 219–232,
1009 doi:10.1016/j.sedgeo.2013.05.016.
- 1010 Li, Z. X. et al., 2008, Assembly, configuration, and break-up history of Rodinia: A synthesis: Precambrian
1011 Research, v. 160, p. 179–210, doi:10.1016/j.precamres.2007.04.021.
- 1012 Loewy, S. L., Connelly, J. N., Dalziel, I. W., and Gower, C. F., 2003, Eastern Laurentia in Rodinia: constraints from
1013 whole-rock Pb and U/Pb geochronology: Tectonophysics, v. 375, p. 169–197, doi:10.1016/s0040-1951(03)00338-x.
- 1014 Lydon, J. W., 2004, Synopsis of the belt-purcell basin: Geological Survey of Canada Mineral Resources Division,
1015 p. 27.
- 1016 Macdonald, F., Halverson, G., Strauss, J., Smith, E., Cox, G., Sperling, E., and Roots, C., 2012, Early
1017 Neoproterozoic basin formation in Yukon, Canada: Implications for the make-up and break-up of Rodinia:
1018 Geoscience Canada, v. 39.
- 1019 Macdonald, F. A., Prave, A. R., Petterson, R., Smith, E. F., Pruss, S. B., Oates, K., Waechter, F., Trotzuk, D., and
1020 Fallick, A. E., 2013, The Laurentian record of Neoproterozoic glaciation, tectonism, and eukaryotic evolution in
1021 Death Valley, California: Geological Society of America Bulletin, v. 125, p. 1203–1223.
- 1022 Macdonald, F. A., Schmitz, M. D., Crowley, J. L., Roots, C. F., Jones, D. S., Maloof, A. C., Strauss, J. V., Cohen,
1023 P. A., Johnston, D. T., and Schrag, D. P., 2010, Calibrating the Cryogenian: Science, v. 327, p. 1241–1243,
1024 doi:10.1126/science.1183325.
- 1025 Macouin, M., Valet, J. P., Besse, J., and Ernst, R. E., 2006, Absolute paleointensity at 1.27 Ga from the Mackenzie
1026 dyke swarm (Canada): Geochem. Geophys. Geosyst., v. 7, p. 10.1029/2005GC000,960.
- 1027 Maloof, A., Halverson, G., Kirschvink, J., Schrag, D., Weiss, B., and Hoffman, P., 2006, Combined paleomagnetic,
1028 isotopic and stratigraphic evidence for true polar wander from the Neoproterozoic Akademikerbreen Group,
1029 Svalbard, Norway: Geological Society of America Bulletin, v. 118, p. 1099–1124, doi:10.1130/B25892.1.

- 1030 Marcussen, C. and Abrahamsen, N., 1983, Palaeomagnetism of the Proterozoic Zig-Zag Dal Basalt and the
1031 Midsommerso Dolerites, eastern North Greenland: Geophysical Journal International, v. 73, p. 367–387,
1032 doi:10.1111/j.1365-246x.1983.tb03321.x.
- 1033 McCausland, P. J. A., Hankard, F., Van der Voo, R., and Hall, C. M., 2011, Ediacaran paleogeography of
1034 Laurentia: Paleomagnetism and 40Ar-39Ar geochronology of the 583 Ma Baie des Moutons syenite, Quebec:
1035 Precambrian Research, v. 187, p. 58–78, doi:10.1016/j.precamres.2011.02.004.
- 1036 McCausland, P. J. A., Van der Voo, R., and Hall, C. M., 2007, Circum-Iapetus paleogeography of the
1037 Precambrian–Cambrian transition with a new paleomagnetic constraint from Laurentia: Precambrian Research,
1038 v. 156, p. 125–152, doi:10.1016/j.precamres.2007.03.004.
- 1039 McFarlane, C. R., 2015, A geochronological framework for sedimentation and Mesoproterozoic tectono-magmatic
1040 activity in lower Belt–Purcell rocks exposed west of Kimberley, British Columbia: Canadian Journal of Earth
1041 Sciences, v. 52, p. 444–465, doi:10.1139/cjes-2014-0215.
- 1042 McGlynn, J. C., Hanson, G. N., Irving, E., and Park, J. K., 1974, Paleomagnetism and age of Nonacho Group
1043 sandstones and associated Sparrow dikes, District of Mackenzie: Canadian Journal of Earth Sciences, v. 11, p.
1044 30–42, doi:10.1139/e74-003.
- 1045 McLelland, J. M., Selleck, B. W., and Bickford, M., 2010, Review of the Proterozoic evolution of the Grenville
1046 Province, its Adirondack outlier, and the Mesoproterozoic inliers of the Appalachians: From Rodinia to Pangea:
1047 The Lithotectonic Record of the Appalachian Region, p. 21–49, doi:10.1130/2010.1206(02).
- 1048 McLelland, J. M., Selleck, B. W., and Bickford, M. E., 2013, Tectonic evolution of the Adirondack Mountains and
1049 Grenville Orogen inliers within the USA: Geoscience Canada, v. 40, p. 318, doi:10.12789/geocanj.2013.40.022.
- 1050 McMechan, M. E. and Price, R. A., 1982, Superimposed low-grade metamorphism in the Mount Fisher area,
1051 southeastern British Columbia—implications for the East Kootenay orogeny: Canadian Journal of Earth
1052 Sciences, v. 19, p. 476–489, doi:10.1139/e82-039.
- 1053 Medig, K., Turner, E., Thorkelson, D., and Rainbird, R., 2016, Rifting of columbia to form a deep-water siliciclastic
1054 to carbonate succession: The mesoproterozoic pinguicula group of northern yukon, canada: Precambrian
1055 Research, v. 278, p. 179–206, doi:10.1016/j.precamres.2016.03.021.
- 1056 Meert, J., der Voo, R. V., and Payne, T., 1994, Paleomagnetism of the Catoctin volcanic province: a new
1057 Vendian-Cambrian apparent polar wander path for North America: Journal of Geophysical Research, v. 99, p.
1058 4625–4641.
- 1059 Meert, J. G. and Stuckey, W., 2002, Revisiting the paleomagnetism of the 1.476 Ga St. Francois Mountains igneous
1060 province, Missouri: Tectonics, v. 21, doi:10.1029/2000tc001265.

- 1061 Merdith, A. S., Collins, A. S., Williams, S. E., Pisarevsky, S., Foden, J. D., Archibald, D. B., Blades, M. L., Alessio,
1062 B. L., Armistead, S., Plavsa, D., and et al., 2017, A full-plate global reconstruction of the Neoproterozoic:
1063 Gondwana Research, v. 50, p. 84–134, doi:10.1016/j.gr.2017.04.001.
- 1064 Met Office, 2010 - 2015, Cartopy: a cartographic python library with a matplotlib interface: Exeter, Devon, URL
1065 <http://scitools.org.uk/cartopy>.
- 1066 Middleton, R. S., Borradaile, G. J., Baker, D., and Lucas, K., 2004, Proterozoic diabase sills of northern Ontario:
1067 Magnetic properties and history: Journal of Geophysical Research: Solid Earth, v. 109,
1068 doi:10.1029/2003jb002581.
- 1069 Mitchell, R. N., Bleeker, W., van Breemen, O., Lecheminant, T. N., Peng, P., Nilsson, M. K. M., and Evans, D.
1070 A. D., 2014, Plate tectonics before 2.0 Ga: Evidence from paleomagnetism of cratons within supercontinent
1071 Nuna: American Journal of Science, v. 314, p. 878–894, doi:10.2475/04.2014.03.
- 1072 Mitchell, R. N., Hoffman, P. F., and Evans, D. A. D., 2010, Coronation loop resurrected: Oscillatory apparent polar
1073 wander of orosirian (2.05–1.8ga) paleomagnetic poles from slave craton: Precambrian Research, v. 179, p.
1074 121–134.
- 1075 Mitchell, R. N., Kilian, T. M., and Evans, D. A. D., 2012, Supercontinent cycles and the calculation of absolute
1076 palaeolongitude in deep time: Nature, v. 482, p. 208–211, doi:10.1038/nature10800.
- 1077 Mosher, S., 1998, Tectonic evolution of the southern laurentian grenville orogenic belt: Geological Society of
1078 America Bulletin, v. 110, p. 1357–1375.
- 1079 Müller, R. D., Cannon, J., Qin, X., Watson, R. J., Gurnis, M., Williams, S., Pfaffelmoser, T., Seton, M., Russell, S.
1080 H. J., and Zahirovic, S., 2018, GPlates: Building a virtual earth through deep time: Geochemistry, Geophysics,
1081 Geosystems, v. 19, p. 2243–2261, doi:10.1029/2018gc007584.
- 1082 Murthy, G., Gower, C., Tubett, M., and Patzold, R., 1992, Paleomagnetism of Eocambrian Long Range dykes and
1083 Double Mer Formation from Labrador, Canada: Canadian Journal of Earth Sciences, v. 29, p. 1224–1234,
1084 doi:10.1139/e92-098.
- 1085 Murthy, G. S., 1978, Paleomagnetic results from the Nain anorthosite and their tectonic implications: Canadian
1086 Journal of Earth Sciences, v. 15, p. 516–525, doi:10.1139/e78-058.
- 1087 Nesheim, T. O., Vervoort, J. D., McClelland, W. C., Gilotti, J. A., and Lang, H. M., 2012, Mesoproterozoic
1088 syntectonic garnet within Belt Supergroup metamorphic tectonites: Evidence of Grenville-age metamorphism
1089 and deformation along northwest Laurentia: Lithos, v. 134–135, p. 91–107, doi:10.1016/j.lithos.2011.12.008.
- 1090 Nimmo, F. and Stevenson, D. J., 2000, Influence of early plate tectonics on the thermal evolution and magnetic
1091 field of Mars: Journal of Geophysical Research: Planets, v. 105, p. 11,969–11,979, doi:10.1029/1999je001216.

- 1092 O'Neill, C., Lenardic, A., and Condie, K. C., 2013, Earth's punctuated tectonic evolution: cause and effect:
1093 Geological Society, London, Special Publications, v. 389, p. 17–40, doi:10.1144/sp389.4.
- 1094 Palin, R. M. and White, R. W., 2015, Emergence of blueschists on Earth linked to secular changes in oceanic crust
1095 composition: *Nature Geoscience*, v. 9, p. 60–64, doi:10.1038/ngeo2605.
- 1096 Palmer, H., 1970, Paleomagnetism and correlation of some Middle Keweenawan rocks, Lake Superior: *Canadian*
1097 *Journal of Earth Science*, v. 7, p. 1410–1436, doi:10.1139/e70-136.
- 1098 Palmer, H. C., Merz, B. A., and Hayatsu, A., 1977, The Sudbury dikes of the Grenville Front region:
1099 paleomagnetism, petrochemistry, and K–Ar age studies: *Canadian Journal of Earth Sciences*, v. 14, p. 1867–1887.
- 1100 Park, J. K., Irving, E., and Donaldson, J. A., 1973, Paleomagnetism of the Precambrian Dubawnt Group:
1101 *Geological Society of America Bulletin*, v. 84, p. 859, doi:10.1130/0016-7606(1973)84<859:potpdg>2.0.co;2.
- 1102 Pehrsson, S. J., Eglington, B. M., Evans, D. A. D., Huston, D., and Reddy, S. M., 2015, Metallogeny and its link to
1103 orogenic style during the Nuna supercontinent cycle: *Geological Society, London, Special Publications*, v. 424,
1104 doi:10.1144/SP424.5.
- 1105 Pérez, F. and Granger, B. E., 2007, IPython: a system for interactive scientific computing: *Computing in Science*
1106 and Engineering, v. 9, p. 21–29, doi:10.1109/MCSE.2007.53.
- 1107 Pesonen, L., 1979, Paleomagnetism of late Precambrian Keweenawan igneous and baked contact rocks from
1108 Thunder Bay district, northern Lake Superior: *Bulletin of the Geological Society of Finland*, v. 51, p. 27–44.
- 1109 Pesonen, L. J. and Halls, H., 1979, The paleomagnetism of Keweenawan dikes from Baraga and Marquette
1110 Counties, northern Michigan: *Canadian Journal of Earth Science*, v. 16, p. 2136–2149, doi:10.1139/e79-201.
- 1111 Piispa, E. J., Smirnov, A. V., Pesonen, L. J., and Mitchell, R. H., 2018, Paleomagnetism and geochemistry of
1112 1144-ma lamprophyre dikes, Northwestern Ontario: Implications for the North American polar wander and plate
1113 velocities: *Journal of Geophysical Research: Solid Earth*, doi:10.1029/2018jb015992.
- 1114 Piper, J., 1992, The palaeomagnetism of major (Middle Proterozoic) igneous complexes, South Greenland and the
1115 Gardar apparent polar wander track: *Precambrian Research*, v. 54, p. 153 – 172,
1116 doi:10.1016/0301-9268(92)90068-Y.
- 1117 Piper, J. and Stearn, J., 1977, Palaeomagnetism of the dyke swarms of the Gardar Igneous Province, south
1118 Greenland: *Physics of the Earth and Planetary Interiors*, v. 14, p. 345–358, doi:10.1016/0031-9201(77)90167-4.
- 1119 Piper, J. D. A., 1977, Palaeomagnetism of the giant dykes of Tugtutoq and Narssaq Gabbro, Gardar Igneous
1120 Province, South Greenland: *Bull. Geol. Soc. Den*, v. 26, p. 85–94.
- 1121 Pisarevsky, S. A., Elming, S.-Å., Pesonen, L. J., and Li, Z.-X., 2014, Mesoproterozoic paleogeography:
1122 Supercontinent and beyond: *Precambrian Research*, v. 244, p. 207–225, doi:10.1016/j.precamres.2013.05.014.

- 1123 Pisarevsky, S. A., Komissarova, R. A., and Khramov, A. N., 2001, Reply to comment by J.G. Meert and R. Van der
1124 Voo on ‘New palaeomagnetic result from Vendian red sediments in Cisbaikalia and the problem of the
1125 relationship of Siberia and Laurentia in the Vendian’: Geophysical Journal International, v. 146, p. 871–873,
1126 doi:10.1046/j.0956-540x.2001.01475.x.
- 1127 Pratt, B. R., 2001, Oceanography, bathymetry and syndepositional tectonics of a precambrian intracratonic basin:
1128 integrating sediments, storms, earthquakes and tsunamis in the belt supergroup (helena formation, ca. 1.45ga),
1129 western north america: Sedimentary Geology, v. 141-142, p. 371–394, doi:10.1016/s0037-0738(01)00083-5.
- 1130 Pratt, B. R. and Ponce, J. J., 2019, Sedimentation, earthquakes, and tsunamis in a shallow, muddy epeiric sea:
1131 Grinnell formation (belt supergroup, ca. 1.45 ga), western north america: GSA Bulletin, v. 131, p. 1411–1439,
1132 doi:10.1130/b35012.1.
- 1133 Prince, J. K. G., 2014, Sequence stratigraphic, lithostratigraphic and stable isotopic analysis of the Minto Inlet
1134 Formation and Kilian Formation of the Shaler Supergroup, Northwest Territories: Master’s thesis, Carleton
1135 University.
- 1136 Pullaiah, G. and Irving, E., 1975, Paleomagnetism of the contact aureole and late dikes of the Otto stock, Ontario,
1137 and its application to early proterozoic apparent polar wandering: Canadian Journal of Earth Sciences, v. 12, p.
1138 1609–1618, doi:10.1139/e75-143.
- 1139 Redden, J., Peterman, Z., Zartman, R., and De-Witt, E., 1990, U-Th-Pb geochronology and preliminary
1140 interpretation of Precambrian tectonic events in the Black Hills, South Dakota: *In The Early Proterozoic*
1141 *Trans-Hudson Orogen*, Geological Association of Canada Special Paper 37, p. 229–251.
- 1142 Rivers, T., 2008, Assembly and preservation of lower, mid, and upper orogenic crust in the Grenville
1143 Province—implications for the evolution of large hot long-duration orogens: Precambrian Research, v. 167, p.
1144 237–259, doi:10.1016/j.precamres.2008.08.005.
- 1145 Robert, B., Besse, J., Blein, O., Greff-Lefftz, M., Baudin, T., Lopes, F., Meslouh, S., and Belbadaoui, M., 2017,
1146 Constraints on the Ediacaran inertial interchange true polar wander hypothesis: A new paleomagnetic study in
1147 Morocco (West African Craton): Precambrian Research, v. 295, p. 90–116, doi:10.1016/j.precamres.2017.04.010.
- 1148 Robert, B., Domeier, M., and Jakob, J., 2020, Iapetan oceans: An analog of tethys?: Geology, doi:10.1130/g47513.1.
- 1149 Robertson, W. and Fahrig, W., 1971, The great Logan Loop - the polar wandering path from Canadian shield rocks
1150 during the Neohelikian era: Canadian Journal of Earth Science, v. 8, p. 1355–1372, doi:10.1139/e71-125.
- 1151 Roest, W. R. and Srivastava, S. P., 1989, Sea-floor spreading in the labrador sea: A new reconstruction: Geology,
1152 v. 17, p. 1000, doi:10.1130/0091-7613(1989)017<1000:sfsitl>2.3.co;2.

- 1153 Rooney, A. D., Austermann, J., Smith, E. F., Li, Y., Selby, D., Dehler, C. M., Schmitz, M. D., Karlstrom, K. E.,
1154 and Macdonald, F. A., 2017, Coupled Re-Os and U-Pb geochronology of the Tonian Chuar Group, Grand
1155 Canyon: *GSA Bulletin*, doi:10.1130/b31768.1.
- 1156 Ross, G. M., 1991, Tectonic setting of the Windermere Supergroup revisited: *Geology*, v. 19, p. 1125,
1157 doi:10.1130/0091-7613(1991)019<1125:tsotws>2.3.co;2.
- 1158 Schmidt, P. W., 1980, Paleomagnetism of igneous rocks from the Belcher Islands, Northwest Territories, Canada:
1159 *Canadian Journal of Earth Sciences*, v. 17, p. 807–822, doi:10.1139/e80-081.
- 1160 Schulz, K. J. and Cannon, W. F., 2007, The Penokean orogeny in the Lake Superior region: *Precambrian Research*,
1161 v. 157, p. 4–25, doi:10.1016/j.precamres.2007.02.022.
- 1162 Schwarz, E. J., Clark, K. R., and Fujiwara, Y., 1982, Paleomagnetism of the Sutton Lake Proterozoic inlier,
1163 Ontario, Canada: *Canadian Journal of Earth Sciences*, v. 19, p. 1330–1332, doi:10.1139/e82-114.
- 1164 Sears, J. W., Chamberlain, K. R., and Buckley, S. N., 1998, Structural and u-pb geochronological evidence for 1.47
1165 ga rifting in the belt basin, western montana: *Canadian Journal of Earth Sciences*, v. 35, p. 467–475,
1166 doi:10.1139/e97-121.
- 1167 Selkin, P. A., Gee, J. S., Meurer, W. P., and Hemming, S. R., 2008, Paleointensity record from the 2.7 Ga Stillwater
1168 Complex, Montana: *Geochem. Geophys. Geosyst.*, v. 9, p. 10.1029/2008GC001,950.
- 1169 Silver, P. G. and Behn, M. D., 2008, Intermittent plate tectonics?: *Science*, v. 319, p. 85–88.
- 1170 Skipton, D. R., St-Onge, M. R., Schneider, D. A., and McFarlane, C. R. M., 2016, Tectonothermal evolution of the
1171 middle crust in the Trans-Hudson Orogen, Baffin Island, Canada: Evidence from petrology and monazite
1172 geochronology of sillimanite-bearing migmatites: *Journal of Petrology*, v. 57, p. 1437–1462,
1173 doi:10.1093/petrology/egw046.
- 1174 Slagstad, T., Culshaw, N. G., Daly, J. S., and Jamieson, R. A., 2009, Western Grenville Province holds key to
1175 midcontinental Granite-Rhyolite Province enigma: *Terra Nova*, v. 21, p. 181–187,
1176 doi:10.1111/j.1365-3121.2009.00871.x.
- 1177 Smith, E. F., Macdonald, F. A., Crowley, J. L., Hodgin, E. B., and Schrag, D. P., 2015, Tectonostratigraphic
1178 evolution of the c. 780–730 Ma Beck Spring Dolomite: Basin Formation in the core of Rodinia: *Geological
1179 Society, London, Special Publications*, v. 424.
- 1180 St-Onge, M. R., Van Gool, J. A. M., Garde, A. A., and Scott, D. J., 2009, Correlation of Archaean and
1181 Palaeoproterozoic units between northeastern Canada and western Greenland: constraining the pre-collisional
1182 upper plate accretionary history of the Trans-Hudson orogen: *Geological Society, London, Special Publications*,
1183 v. 318, p. 193–235, doi:10.1144/sp318.7.

- 1184 Stern, R. J. and Miller, N. R., 2018, Did the transition to plate tectonics cause neoproterozoic snowball earth?:
1185 *Terra Nova*, v. 30, p. 87–94, doi:10.1111/ter.12321.
- 1186 Stern, R. J., Tsujimori, T., Harlow, G., and Groat, L. A., 2013, Plate tectonic gemstones: *Geology*, v. 41, p.
1187 723–726, doi:10.1130/g34204.1.
- 1188 Swanson-Hysell, N. L., Burgess, S. D., Maloof, A. C., and Bowring, S. A., 2014a, Magmatic activity and plate
1189 motion during the latent stage of Midcontinent Rift development: *Geology*, v. 42, p. 475–478,
1190 doi:10.1130/G35271.1.
- 1191 Swanson-Hysell, N. L., Maloof, A. C., Condon, D. J., Jenkin, G. R. T., Alene, M., Tremblay, M. M., Tesema, T.,
1192 Rooney, A. D., and Haileab, B., 2015, Stratigraphy and geochronology of the Tambien Group, Ethiopia:
1193 Evidence for globally synchronous carbon isotope change in the Neoproterozoic: *Geology*, doi:10.1130/G36347.1.
- 1194 Swanson-Hysell, N. L., Ramezani, J., Fairchild, L. M., and Rose, I. R., 2019, Failed rifting and fast drifting:
1195 Midcontinent Rift development, Laurentia's rapid motion and the driver of Grenvillian orogenesis: *GSA Bulletin*,
1196 doi:10.1130/b31944.1.
- 1197 Swanson-Hysell, N. L., Vaughan, A. A., Mustain, M. R., and Asp, K. E., 2014b, Confirmation of progressive plate
1198 motion during the Midcontinent Rift's early magmatic stage from the Osler Volcanic Group, Ontario, Canada:
1199 *Geochemistry Geophysics Geosystems*, v. 15, p. 2039–2047, doi:10.1002/2013GC005180.
- 1200 Symons, D. and Chiasson, A., 1991, Paleomagnetism of the Callander Complex and the Cambrian apparent polar
1201 wander path for North America: *Canadian Journal of Earth Science*, v. 1991, p. 355–363, doi:10.1139/e91-032.
- 1202 Symons, D., Symons, T., and Lewchuk, M., 2000, Paleomagnetism of the Deschambault pegmatites: Stillstand and
1203 hairpin at the end of the Paleoproterozoic Trans-Hudson Orogeny, Canada: *Physics and Chemistry of the Earth*,
1204 Part A: Solid Earth and Geodesy, v. 25, p. 479–487, doi:10.1016/s1464-1895(00)00074-0.
- 1205 Symons, D. T. A. and Mackay, C. D., 1999, Paleomagnetism of the Boot-Phantom pluton and the amalgamation of
1206 the juvenile domains in the Paleoproterozoic Trans-Hudson Orogen, Canada: In Sinha, A. K., ed., *Basement
1207 Tectonics 13*, Springer Netherlands, Dordrecht, p. 313–331, doi:10.1007/978-94-011-4800-9__18.
- 1208 Tanczyk, E., Lapointe, P., Morris, W., and Schmidt, P., 1987, A paleomagnetic study of the layered mafic intrusions
1209 at Sept-Iles, Quebec: *Canadian Journal of Earth Science*, v. 24, p. 1431–1438, doi:10.1139/e87-135.
- 1210 Tauxe, L. and Kodama, K., 2009, Paleosecular variation models for ancient times: Clues from Keweenawan lava
1211 flows: *Physics of the Earth and Planetary Interiors*, v. 177, p. 31–45, doi:10.1016/j.pepi.2009.07.006.
- 1212 Tauxe, L., Shaar, R., Jonestrask, L., Swanson-Hysell, N., Minnett, R., Koppers, A., Constable, C., Jarboe, N.,
1213 Gaastra, K., and Fairchild, L., 2016, PmagPy: Software package for paleomagnetic data analysis and a bridge to
1214 the Magnetics Information Consortium (MagIC) Database: *Geochemistry, Geophysics, Geosystems*,
1215 doi:10.1002/2016GC006307.

- 1216 Torsvik, T. H. and Cocks, L. R. M., 2017, Earth history and palaeogeography: Cambridge University Press,
1217 doi:10.1017/9781316225523.
- 1218 Torsvik, T. H., van der Voo, R., Doubrovine, P. V., Burke, K., Steinberger, B., Ashwal, L. D., Trønnes, R. G.,
1219 Webb, S. J., and Bull, A. L., 2014, Deep mantle structure as a reference frame for movements in and on the
1220 Earth: Proceedings of the National Academy of Sciences, doi:10.1073/pnas.1318135111.
- 1221 Torsvik, T. H., Van der Voo, R., Preeden, U., Mac Niocaill, C., Steinberger, B., Doubrovine, P. V., van Hinsbergen,
1222 D. J. J., Domeier, M., Gaina, C., Tohver, E., Meert, J. G., McCausland, P. J. A., and Cocks, L. R. M., 2012,
1223 Phanerozoic polar wander, palaeogeography and dynamics: Earth-Science Reviews, v. 114, p. 325–368,
1224 doi:10.1016/j.earscirev.2012.06.007.
- 1225 Turner, E. C. and Bekker, A., 2016, Thick sulfate evaporite accumulations marking a mid-neoproterozoic
1226 oxygenation event (ten stone formation, northwest territories, canada): Geological Society of America Bulletin,
1227 v. 128, p. 203–222.
- 1228 Veikkolainen, T., Pesonen, L., and Evans, D. A. D., 2014, PALEOMAGIA: A PHP/MYSQL database of the
1229 Precambrian paleomagnetic data: Studia Geophysica et Geodaetica, p. 1–17, doi:10.1007/s11200-013-0382-0.
- 1230 Verbaas, J., Thorkelson, D. J., Milidragovic, D., Crowley, J. L., Foster, D., Daniel Gibson, H., and Marshall, D. D.,
1231 2018, Rifting of western laurentia at 1.38 ga: The hart river sills of yukon, canada: Lithos, v. 316-317, p.
1232 243–260, doi:10.1016/j.lithos.2018.06.018.
- 1233 Wang, C.-C., Jacobs, J., Elburg, M. A., Läufer, A., Thomas, R. J., and Elvevold, S., 2020, Grenville-age continental
1234 arc magmatism and crustal evolution in central dronning maud land (east antarctica): Zircon geochronological
1235 and hf-o isotopic evidence: Gondwana Research, v. 82, p. 108–127, doi:10.1016/j.gr.2019.12.004.
- 1236 Warnock, A., Kodama, K., and Zeitler, P., 2000, Using thermochronometry and low-temperature demagnetization
1237 to accurately date Precambrian paleomagnetic poles: Journal of Geophysical Research, v. 105, p. 19,435–19,453,
1238 doi:10.1029/2000jb900114.
- 1239 Weil, A., Geissman, J., Heizler, M., and Van der Voo, R., 2003, Paleomagnetism of Middle Proterozoic mafic
1240 intrusions and Upper Proterozoic (Nankoweap) red beds from the Lower Grand Canyon Supergroup, Arizona:
1241 Tectonophysics, v. 375, p. 199–220, doi:10.1016/S0040-1951(03)00339-1.
- 1242 Weil, A. B., Geissman, J. W., and Ashby, J. M., 2006, A new paleomagnetic pole for the Neoproterozoic Uinta
1243 Mountain supergroup, Central Rocky Mountain States, USA: Precambrian Research, v. 147, p. 234–259,
1244 doi:10.1016/j.precamres.2006.01.017.
- 1245 Weil, A. B., Geissman, J. W., and Voo, R. V. d., 2004, Paleomagnetism of the Neoproterozoic Chuar Group, Grand
1246 Canyon Supergroup, Arizona: implications for Laurentia's Neoproterozoic APWP and Rodinia break-up:
1247 Precambrian Research, v. 129, p. 71–92.

- 1248 Weller, O. M. and St-Onge, M. R., 2017, Record of modern-style plate tectonics in the Palaeoproterozoic
 1249 Trans-Hudson orogen: *Nature Geoscience*, v. 10, doi:10.1038/ngeo2904.
- 1250 White, B., 1984, Stromatolites and associated facies in shallowing-upward cycles from the middle proterozoic altyn
 1251 formation of glacier national park, montana: *Precambrian Research*, v. 24, p. 1–26,
 1252 doi:10.1016/0301-9268(84)90067-6.
- 1253 Whitmeyer, S. and Karlstrom, K., 2007, Tectonic model for the Proterozoic growth of North America: *Geosphere*,
 1254 v. 3, p. 220–259, doi:10.1130/GES00055.1.
- 1255 WINSTON, D., 2007, Revised stratigraphy and depositional history of the helena and wallace formations,
 1256 mid-proterozoic piegan group, belt supergroup, montana and idaho, u.s.a.: *In Proterozoic Geology of Western*
 1257 *North America and Siberia*, SEPM (Society for Sedimentary Geology), p. 65–100, doi:10.2110/pec.07.86.0065,
 1258 URL <https://doi.org/10.2110%2Fpec.07.86.0065>.
- 1259 Witkosky, R. and Wernicke, B. P., 2018, Subsidence history of the Ediacaran Johnnie Formation and related strata
 1260 of southwest Laurentia: Implications for the age and duration of the Shuram isotopic excursion and animal
 1261 evolution: *Geosphere*, v. 14, p. 2245–2276, doi:10.1130/ges01678.1.
- 1262 Yonkee, W., Dehler, C., Link, P., Balgord, E., Keeley, J., Hayes, D., Wells, M., Fanning, C., and Johnston, S., 2014,
 1263 Tectono-stratigraphic framework of neoproterozoic to cambrian strata, west-central u.s.: Protracted rifting,
 1264 glaciation, and evolution of the north american cordilleran margin: *Earth-Science Reviews*, v. 136, p. 59–95,
 1265 doi:10.1016/j.earscirev.2014.05.004.
- 1266 Zhang, S., Li, Z.-X., Evans, D. A. D., Wu, H., Li, H., and Dong, J., 2012, Pre-Rodinia supercontinent Nuna shaping
 1267 up: A global synthesis with new paleomagnetic results from North China: *Earth and Planetary Science Letters*,
 1268 v. 353–354, p. 145–155, doi:10.1016/j.epsl.2012.07.034.
- 1269 Zhao, H., Zhang, S., Ding, J., Chang, L., Ren, Q., Li, H., Yang, T., and Wu, H., 2019, New geochronologic and
 1270 paleomagnetic results from early neoproterozoic mafic sills and late mesoproterozoic to early neoproterozoic
 1271 successions in the eastern north china craton, and implications for the reconstruction of rodinia: *GSA Bulletin*,
 1272 doi:10.1130/b35198.1.

Table 1. Rotations of separated terranes

Block	Euler pole longitude	Euler pole latitude	rotation angle	note and citation
Greenland	-118.5	67.5	-13.8	Cenozoic separation of Greenland from Laurentia associated with opening of Baffin Bay and the Labrador Sea (Roest and Srivastava, 1989)
Scotland	161.9	78.6	-31.0	Reconstructing Atlantic opening following Torsvik and Cocks (2017)
Svalbard	125.0	-81.0	68	Rotate Svalbard to Laurentia in fit that works well with East Greenland basin according to Maloof et al. (2006)

Table 2: Compilation of paleomagnetic poles from Laurentia

terrane	unit name	Nordic rating	site lon (°)	site lat (°)	plon (°)	plat (°)	A ₉₅ (°)	age (Ma)	pole reference
Laurentia-Wyoming	Stillwater Complex - C2	A	249.2	45.2	335.8	-83.6	4.0	2705 ⁺⁴ ₋₄	Selkin et al. (2008)
Laurentia-Superior(East)	Otto Stock dykes and aureole	B	279.9	48.0	227.0	69.0	4.8	2676 ⁺⁵ ₋₅	Pullaiah and Irving (1975)
Laurentia-Slave	Defeat Suite	B	245.5	62.5	64.0	-1.0	15.0	2625 ⁺⁵ ₋₅	Mitchell et al. (2014)
Laurentia-Superior(East)	Ptarmigan-Mistassini dykes	B	287.0	54.0	213.0	-45.3	13.8	2505 ⁺² ₋₂	Evans and Halls (2010)
Laurentia-Superior(East)	Matachewan dykes R	A	278.0	48.0	238.3	-44.1	1.6	2466 ⁺²³ ₋₂₃	Evans and Halls (2010)
Laurentia-Superior(East)	Matachewan dykes N	A	278.0	48.0	239.5	-52.3	2.4	2446 ⁺³ ₋₃	Evans and Halls (2010)
Laurentia-Slave	Malley dykes	A	249.8	64.2	310.0	-50.8	6.7	2231 ⁺² ₋₂	Buchan et al. (2012)
Laurentia-Superior(East)	Senneterre dykes	A	283.0	49.0	284.3	-15.3	5.5	2218 ⁺⁶ ₋₆	Buchan et al. (1993)
Laurentia-Superior(East)	Nipissing N1 sills	A	279.0	47.0	272.0	-17.0	10.0	2217 ⁺⁴ ₋₄	Buchan et al. (2000)
Laurentia-Slave	Dogrib dykes	A	245.5	62.5	315.0	-31.0	7.0	2193 ⁺² ₋₂	Mitchell et al. (2014)
Laurentia-Superior(East)	Biscotasing dykes	A	280.0	48.0	223.9	26.0	7.0	2170 ⁺³ ₋₃	Evans and Halls (2010)
Laurentia-Wyoming	Rabbit Creek, Powder River and South Path Dykes	A	252.8	43.9	339.2	65.5	7.6	2160 ⁺¹¹ ₋₈	Kilian et al. (2015)
Laurentia-Slave	Indin dykes	A	245.6	62.5	256.0	-36.0	7.0	2126 ⁺³ ₋₁₈	Buchan et al. (2016)
Laurentia-Superior(West)	Marathon dykes N	A	275.0	49.0	198.2	45.4	7.7	2124 ⁺³ ₋₃	Halls et al. (2008)

Continued on next page

terrane	unit name	Nordic rating	site lon (°)	site lat (°)	plon (°)	plat (°)	A ₉₅ (°)	age (Ma)	pole reference
Laurentia-Superior(West)	Marathon dykes R	A	275.0	49.0	182.2	55.1	7.5	2104 ⁺³ ₋₃	Halls et al. (2008)
Laurentia-Superior(West)	Cauchon Lake dykes	A	263.0	56.0	180.9	53.8	7.7	2091 ⁺² ₋₂	Evans and Halls (2010)
Laurentia-Superior(West)	Fort Frances dykes	A	266.0	48.0	184.6	42.8	6.1	2077 ⁺⁵ ₋₅	Evans and Halls (2010)
Laurentia-Superior(East)	Lac Esprit dykes	A	282.0	53.0	170.5	62.0	6.4	2069 ⁺¹ ₋₁	Evans and Halls (2010)
Laurentia-Greenland-Nain	Kangamiut Dykes	B	307.0	66.0	273.8	17.1	2.7	2042 ⁺¹² ₋₁₂	Fahrig and Bridgwater (1976)
Laurentia-Slave	Lac de Gras dykes	A	249.6	64.4	267.9	11.8	7.1	2026 ⁺⁵ ₋₅	Buchan et al. (2009)
Laurentia-Superior(East)	Minto dykes	A	285.0	57.0	171.5	38.7	13.1	1998 ⁺² ₋₂	Evans and Halls (2010)
Laurentia-Slave	Rifle Formation	B	252.9	65.9	341.0	14.0	7.7	1963 ⁺⁶ ₋₆	Evans and Hoye (1981)
Laurentia-Rae	Clearwater Anorthosite	B	251.6	57.1	311.8	6.5	2.9	1917 ⁺⁷ ₋₇	Halls and Hanes (1999)
Laurentia-Wyoming	Sourdough mafic dike swarm	A	-108.3	44.7	292.0	49.2	8.1	1899 ⁺⁵ ₋₅	Kilian et al. (2016)
Laurentia-Slave	Ghost Dike Swarm	A	244.6	62.6	286.0	-2.0	6.0	1887 ⁺⁵ ₋₉	Buchan et al. (2016)
Laurentia-Slave	Mean Se-ton/Akaitcho/Mara	B	250.0	65.0	260.0	-6.0	4.0	1885 ⁺⁵ ₋₅	Mitchell et al. (2010)
Laurentia-Slave	Mean Kahochella, Peacock Hills	B	250.0	65.0	285.0	-12.0	7.0	1882 ⁺⁴ ₋₄	Mitchell et al. (2010)
Laurentia-Superior(West)	Molson (B+C2) dykes	A	262.0	55.0	218.0	28.9	3.8	1879 ⁺⁶ ₋₆	Evans and Halls (2010)

Continued on next page

terrane	unit name	Nordic rating	site lon (°)	site lat (°)	plon (°)	plat (°)	A ₉₅ (°)	age (Ma)	pole reference
Laurentia-Slave	Douglas Peninsula Formation, Pethei Group	B	249.7	62.8	258.0	-18.0	14.2	1876 ⁺¹⁰ ₋₁₀	Irving and McGlynn (1979)
Laurentia-Slave	Takiyuak Formation	B	246.9	66.1	249.0	-13.0	8.0	1876 ⁺¹⁰ ₋₁₀	Irving and McGlynn (1979)
Laurentia-Superior	Haig/Flaherty/Sutton Mean	B	279.0	56.0	245.8	1.0	3.9	1870 ⁺¹ ₋₁	Nordic workshop calculation based on data of Schmidt (1980); Schwarz et al. (1982)
Laurentia-Slave	Pearson A/Peninsular/Kilohigok sills	A	250.0	65.0	269.0	-22.0	6.0	1870 ⁺⁴ ₋₄	Mitchell et al. (2010)
Laurentia-Trans-Hudson orogen	Boot-Phantom Pluton	B	258.1	54.7	275.4	62.4	7.9	1838 ⁺¹ ₋₁	Symons and Mackay (1999)
Laurentia-Rae	Sparrow Dykes	B	250.2	61.6	291.0	12.0	7.9	1827 ⁺⁴ ₋₄	McGlynn et al. (1974)
Laurentia-Rae	Martin Formation	A	251.4	59.6	288.0	-9.0	8.5	1818 ⁺⁴ ₋₄	Evans and Bingham (1973)
Laurentia	Dubawnt Group	B	265.6	64.1	277.0	7.0	8.0	1785 ⁺³⁵ ₋₃₅	Park et al. (1973)
Laurentia-Trans-Hudson orogen	Deschambault Pegmatites	B	256.7	54.9	276.0	67.5	7.7	1766 ⁺⁵ ₋₅	Symons et al. (2000)
Laurentia-Trans-Hudson orogen	Jan Lake Granite	B	257.2	54.9	264.3	24.3	16.9	1758 ⁺¹ ₋₁	Gala et al. (1995)
Laurentia	Cleaver Dykes	A	242.0	67.5	276.7	19.4	6.1	1741 ⁺⁵ ₋₅	Irving (2004)
Laurentia-Greenland	Melville Bugt dia-base dykes	B	303.0	74.6	273.8	5.0	8.7	1633 ⁺⁵ ₋₅	Halls et al. (2011)
Laurentia	Western Channel Diabase	A	242.2	66.4	245.0	9.0	6.6	1590 ⁺³ ₋₃	Irving and Park (1972)

Continued on next page

terrane	unit name	Nordic rating	site lon (°)	site lat (°)	plon (°)	plat (°)	A ₉₅ (°)	age (Ma)	pole reference
Laurentia	St.Francois Mountains Acidic Rocks	A	269.5	37.5	219.0	-13.2	6.1	1476 ⁺¹⁶ ₋₁₆	Meert and Stuckey (2002)
Laurentia	Michikamau Intrusion	A	296.0	54.5	217.5	-1.5	4.7	1460 ⁺⁵ ₋₅	Emslie et al. (1976)
Laurentia	Spokane Formation	A	246.8	48.2	215.5	-24.8	4.7	1458 ⁺¹³ ₋₁₃	Elston et al. (2002)
Laurentia	Snowslip Formation	A	245.9	47.9	210.2	-24.9	3.5	1450 ⁺¹⁴ ₋₁₄	Elston et al. (2002)
Laurentia	Tobacco Root dykes	B	247.6	47.4	216.1	8.7	10.5	1448 ⁺⁴⁹ ₋₄₉	Harlan et al. (2008)
Laurentia	Purcell Lava	A	245.1	49.4	215.6	-23.6	4.8	1443 ⁺⁷ ₋₇	Elston et al. (2002)
Laurentia	Rocky Mountain intrusions	B	253.8	40.3	217.4	-11.9	9.7	1430 ⁺¹⁵ ₋₁₅	Nordic workshop calculation based on data of Harlan et al. (1994); Harlan and Geissman (1998)
Laurentia	Mistastin Pluton	B	296.3	55.6	201.5	-1.0	7.6	1425 ⁺²⁵ ₋₂₅	Fahrig and Jones (1976)
Laurentia	McNamara Formation	A	246.4	46.9	208.3	-13.5	6.7	1401 ⁺⁶ ₋₆	Elston et al. (2002)
Laurentia	Pilcher, Garnet Range and Libby Formations	A	246.4	46.7	215.3	-19.2	7.7	1385 ⁺²³ ₋₂₃	Elston et al. (2002)
Laurentia-Greenland	Zig-Zag Dal Basalts	B	334.8	81.2	242.8	12.0	3.8	1382 ⁺² ₋₂	Marcussen and Abrahamsen (1983)
Laurentia-Greenland	Midsommersoe Dolerite	B	333.4	81.6	242.0	6.9	5.1	1382 ⁺² ₋₂	Marcussen and Abrahamsen (1983)
Laurentia-Greenland	Victoria Fjord dolerite dykes	B	315.3	81.5	231.7	10.3	4.3	1382 ⁺² ₋₂	Abrahamsen and Van Der Voo (1987)

Continued on next page

terrane	unit name	Nordic rating	site lon (°)	site lat (°)	plon (°)	plat (°)	A_{95} (°)	age (Ma)	pole reference
Laurentia	Nain Anorthosite	B	298.2	56.5	206.7	11.7	2.2	1305^{+15}_{-15}	Murthy (1978)
Laurentia-Greenland	North Qoroq intrusives	B	314.6	61.1	202.6	13.2	8.3	1275^{+1}_{-1}	Piper (1992)
Laurentia-Greenland	Kungnat Ring Dyke	B	311.7	61.2	198.7	3.4	3.2	1275^{+2}_{-2}	Piper and Stearn (1977)
Laurentia	Mackenzie dykes	A	250.0	65.0	190.0	4.0	5.0	1267^{+2}_{-2}	Buchan et al. (2000)
	grand mean								
Laurentia-Greenland	West Gardar Dolerite Dykes	B	311.7	61.2	201.7	8.7	6.6	1244^{+8}_{-8}	Piper and Stearn (1977)
Laurentia-Greenland	West Gardar Lamprophyre Dykes	B	311.7	61.2	206.4	3.2	7.2	1238^{+11}_{-11}	Piper and Stearn (1977)
Laurentia	Sudbury Dykes	A	278.6	46.3	192.8	-2.5	2.5	1237^{+5}_{-5}	Palmer et al. (1977)
	Combined								
Laurentia-Scotland	Stoer Group	B	354.5	58.0	238.4	37.2	7.7	1199^{+70}_{-70}	Nordic workshop calculation
Laurentia-Greenland	Narssaq Gabbro	B	313.8	60.9	225.4	31.6	9.7	1184^{+5}_{-5}	Piper (1977)
Laurentia-Greenland	Hviddal Giant Dyke	B	313.7	60.9	215.3	33.2	9.6	1184^{+5}_{-5}	Piper (1977)
Laurentia-Greenland	South Qoroq Intr.	A	314.6	61.1	215.9	41.8	13.1	1163^{+2}_{-2}	Piper (1992)
Laurentia-Greenland	Giant Gabbro Dykes	B	313.7	60.9	226.1	42.3	9.4	1163^{+2}_{-2}	Piper (1977)
Laurentia-Greenland	NE-SW Trending dykes	B	314.6	61.1	230.8	33.4	5.7	1160^{+5}_{-5}	Piper (1992)
Laurentia	Ontario lamprophyre dykes	NR	273.3	48.8	223.3	58.0	9.2	1143^{+10}_{-10}	Piispa et al. (2018)

Continued on next page

terrane	unit name	Nordic rating	site lon (°)	site lat (°)	plon (°)	plat (°)	A_{95} (°)	age (Ma)	pole reference
Laurentia	Abitibi Dykes	A	279.0	48.0	215.5	48.8	14.1	1141^{+2}_{-2}	Ernst and Buchan (1993)
Laurentia	Nipigon sills and lavas	A	270.9	49.1	217.8	47.2	4.0	1109^{+2}_{-2}	Nordic workshop calculation based on data of Palmer (1970); Robertson and Fahrig (1971); Pesonen (1979); Pesonen and Halls (1979); Middleton et al. (2004); Borradaile and Middleton (2006)
Laurentia	Lowermost Mamainse Point volcanics -R1	A	275.3	47.1	227.0	49.5	5.3	1109^{+2}_{-3}	Swanson-Hysell et al. (2014a)
Laurentia	Lower Osler volcanics -R	A	272.3	48.8	218.6	40.9	4.8	1108^{+3}_{-3}	Swanson-Hysell et al. (2014b)
Laurentia	Middle Osler volcanics -R	A	272.4	48.8	211.3	42.7	8.2	1107^{+4}_{-4}	Swanson-Hysell et al. (2014b)
Laurentia	Upper Osler volcanics -R	A	272.4	48.7	203.4	42.3	3.7	1105^{+1}_{-1}	Halls (1974); Swanson-Hysell et al. (2014b, 2019)
Laurentia	Lower Mamainse Point volcanics -R2	A	275.3	47.1	205.2	37.5	4.5	1105^{+3}_{-4}	Swanson-Hysell et al. (2014a)
Laurentia	Mamainse Point volcanics -C (lower N, upper R)	A	275.3	47.1	189.7	36.1	4.9	1101^{+1}_{-1}	Swanson-Hysell et al. (2014a)
Laurentia	North Shore lavas -N	A	268.7	46.3	181.7	31.1	2.1	1097^{+3}_{-3}	Tauxe and Kodama (2009); Swanson-Hysell et al. (2019)

Continued on next page

terrane	unit name	Nordic rating	site lon (°)	site lat (°)	plon (°)	plat (°)	A ₉₅ (°)	age (Ma)	pole reference
Laurentia	Portage Lake Volcanics	A	271.2	47.0	182.5	27.5	2.3	1095 ₋₃ ⁺³	Books (1972); Hnat et al. (2006) as calculated in Swanson-Hysell et al. (2019)
Laurentia	Chengwatana Volcanics	B	267.3	45.4	186.1	30.9	8.2	1095 ₋₂ ⁺²	Kean et al. (1997)
Laurentia	Uppermost Mainse Point volcanics -N	A	275.3	47.1	183.2	31.2	2.5	1094 ₋₄ ⁺⁶	Swanson-Hysell et al. (2014a)
Laurentia	Cardenas Basalts and Intrusions	B	248.1	36.1	185.0	32.0	8.0	1091 ₋₅ ⁺⁵	Weil et al. (2003)
Laurentia	Schroeder Lutsen Basalts	A	269.1	47.5	187.8	27.1	3.0	1090 ₋₇ ⁺²	Fairchild et al. (2017)
Laurentia	Central Arizona diabases -N	A	249.2	33.7	175.3	15.7	7.0	1088 ₋₁₁ ⁺¹¹	Donadini et al. (2011)
Laurentia	Lake Shore Traps	A	271.9	47.6	186.4	23.1	4.0	1086 ₋₁ ⁺¹	Kulakov et al. (2013)
Laurentia	Michipicoten Island Formation	A	274.3	47.7	174.7	17.0	4.4	1084 ₋₁ ⁺¹	Fairchild et al. (2017)
Laurentia	Nonesuch Shale	B	271.5	47.0	178.1	7.6	5.5	1080 ₋₁₀ ⁺⁴	Henry et al. (1977)
Laurentia	Freda Sandstone	B	271.5	47.0	179.0	2.2	4.2	1070 ₋₁₀ ⁺¹⁴	Henry et al. (1977)
Laurentia	Haliburton Intrusions	B	281.4	45.0	141.9	-32.6	6.3	1015 ₋₁₅ ⁺¹⁵	Warnock et al. (2000)
Laurentia-Scotland	Torridon Group	B	354.3	57.9	220.9	-17.7	7.1	925 ₋₁₄₅ ⁺¹⁴⁵	Nordic workshop calculation
Laurentia-Svalbard	Lower Grusdievbreen Formation	B	18.0	79.0	204.9	19.6	10.9	831 ₋₂₀ ⁺²⁰	Maloof et al. (2006)

Continued on next page

terrane	unit name	Nordic rating	site lon (°)	site lat (°)	plon (°)	plat (°)	A ₉₅ (°)	age (Ma)	pole reference
Laurentia-Svalbard	Upper Grus-dievbreen Formation	B	18.2	78.9	252.6	-1.1	6.2	800 ⁺¹¹ ₋₁₁	Maloof et al. (2006)
Laurentia	Gunbarrel dykes	B	248.7	44.8	138.2	9.1	12.0	778 ⁺² ₋₂	Calculation from Eyster et al. (2019) based on data of Harlan (1993); Harlan et al. (1997)
Laurentia-Svalbard	Svanbergfjellet Formation	B	18.0	78.5	226.8	25.9	5.8	770 ⁺¹⁹ ₋₄₀	Maloof et al. (2006)
Laurentia	Uinta Mountain Group	B	250.7	40.8	161.3	0.8	4.7	760 ⁺⁶ ₋₁₀	Weil et al. (2006)
Laurentia	Carbon Canyon	NR	248.2	36.1	166.0	-0.5	9.7	757 ⁺⁷ ₋₇	Weil et al. (2004) as calculated in Eyster et al. (2019)
Laurentia	Carbon Butte/Awatubi	NR	248.5	35.2	163.8	14.2	3.5	751 ⁺⁸ ₋₈	Eyster et al. (2019)
Laurentia	Franklin event grand mean	A	275.4	73.0	162.1	6.7	3.0	724 ⁺³ ₋₃	Denyszyn et al. (2009a)
Laurentia	Long Range Dykes	B	303.3	53.7	175.3	-19.0	17.4	615 ⁺² ₋₂	Murthy et al. (1992)
Laurentia	Baie des Moutons complex (A)	B	301.0	50.8	152.7	-42.6	12.0	583 ⁺² ₋₂	McCausland et al. (2011)
Laurentia	Baie des Moutons complex (B)	B	301.0	50.8	141.5	34.2	15.4	583 ⁺² ₋₂	McCausland et al. (2011)
Laurentia	Callander Alkaline Complex	B	280.6	46.2	121.4	-46.3	6.0	575 ⁺⁵ ₋₅	Symons and Chiasson (1991)
Laurentia	Catoctin Basalts	B	281.8	38.5	116.7	-42.0	17.5	572 ⁺⁵ ₋₅	Meert et al. (1994)

Continued on next page

terrane	unit name	Nordic rating	site lon (°)	site lat (°)	plon (°)	plat (°)	A ₉₅ (°)	age (Ma)	pole reference
Laurentia	Sept-Iles layered intrusion	B	293.5	50.2	141.0	20.0	6.7	565 ⁺⁴ ₋₄	Tanczyk et al. (1987)